Available online at www.sciencedirect.com
SCIENCE DIRECT®
Precambrian Research 122 (2003) 85–109
Precambrian Research
www.elsevier.com/locate/precamres

Geochronology of Neoproterozoic syn-rift magmatism in the Yangtze Craton, South China and correlations with other continents: evidence for a mantle superplume that broke up Rodinia

Z.X. Li [a,*], X.H. Li [b], P.D. Kinny [c], J. Wang [d], S. Zhang [e], H. Zhou [f]

[a] *Tectonics Special Research Centre, School of Earth and Geographical Sciences, The University of Western Australia, Crawley, WA 6009, Australia*
[b] *Guangzhou Institute of Geochemistry, Chinese Academy of Sciences, PO Box 1131, Guangzhou, China*
[c] *Department of Applied Geology, Tectonics Special Research Centre, Curtin University of Technology, Perth, WA 6845, Australia*
[d] *Chengdu Institute of Geology and Mineral Resources, China Geological Survey, Chengdu 610082, China*
[e] *School of Earth and Land Resources, China University of Geosciences, Beijing 10083, China*
[f] *Faculty of Earth Sciences, China University of Geosciences, Lumo Road 31,Wuhan 430074, Hubei, China*

Received 18 February 2002; received in revised form 18 February 2002; accepted 5 June 2002

Abstract

Neoproterozoic granitic intrusions in South China have traditionally been interpreted as related to orogenesis, marking the cratonisation of the Yangtze Block. However, a number of ca. 830–820 Ma granitoids and mafic–ultramafic intrusions unconformably overlain by Neoproterozoic rift successions have recently been reinterpreted as being related to a mantle plume during the breakup of the supercontinent Rodinia. In this paper, we report SHRIMP zircon U–Pb ages from granitoids and gabbros that are closely related to the Neoproterozoic rifting event, and one age from a volcanic unit in the rift successions. We demonstrate that there were two major phases of widespread bimodal magmatism in South China during the Neoproterozoic. The first one, at ca. 830–795 Ma, started before the continental rift but continued into the first two stages of the rifting. The second one, ca. 780–745 Ma, occurred during the later stages of the rifting. Some co-magmatic mafic dykes have rare-earth element and trace element distribution characteristic of continental flood basalts. Similar age patterns of Neoproterozoic anorogenic magmatism are recorded in most other Rodinian continental blocks, such as Australia, India, Madagascar, Seychelles, southern Africa and Laurentia. The widespread occurrence and protracted duration (ca. 85 million years) of such anorogenic magmatism require a large and sustained heat source. We interpret these magmatism as results of a mantle superplume beneath Rodinia, which was responsible for the breakup of the supercontinent during the Neoproterozoic.

Keywords: South China; Rodinia; Neoproterozoic; Magmatism; Mantle plume; Superplume

1. Introduction

Anderson (1982) first observed the close spatial and temporal relationships between the palaeogeographic position of the supercontinent Pangaea, the

* Corresponding author. Tel.: +61-8-9380-2652; fax: +61-8-9380-1037.
E-mail address: zli@tsrc.uwa.edu.au (Z.X. Li).

0301-9268/02/$ – see front matter © 2002 Elsevier Science B.V. All rights reserved.
PII: S0301-9268(02)00208-5

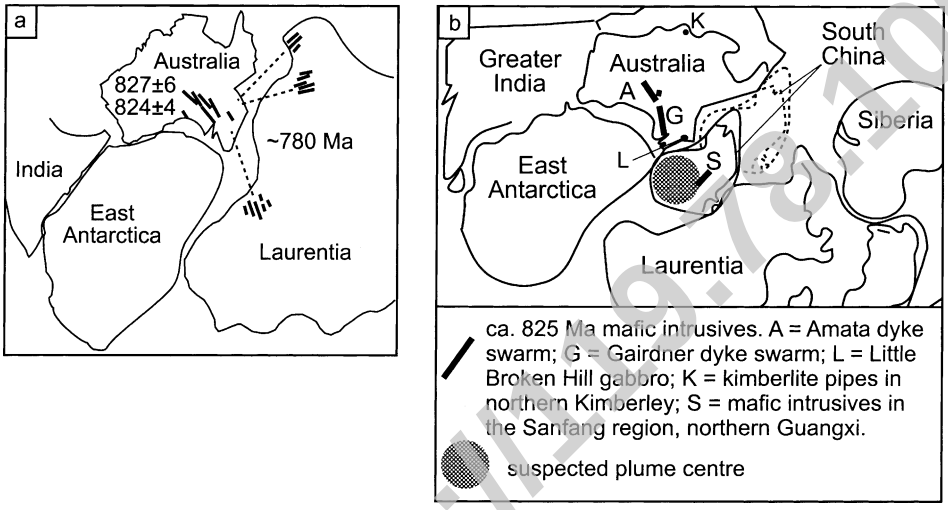

Fig. 1. Ca. 780 Ma ((a) after Park et al., 1995) and 825 Ma ((b) after Li et al., 1999) mantle plumes previously proposed under Rodinia. See text for sources of ages.

position of the present Atlantic–African geoid high, and a concentration of hotspots. He hypothesised that "*the pent-up heat*" beneath the supercontinent "*causes rifts and hotspots and results in uplift, magmatism, fragmentation and dispersal of the continents*". Many of Anderson's predictions were verified by later workers, such as the existence of extensive intercontinental magmatism over Pangaea prior to its breakup (e.g. Doblas et al., 1998). However, these later workers commonly invoked a mantle superplume, rather than Anderson's (1994) upper-mantle upwelling, as the most likely cause of the phenomena they observed at the Earth's surface. Recent global seismic tomography data (e.g. Zhao, 2001) demonstrate the core-mantle boundary origin of large areas of abnormally hot mantle, which could be residua of the Pangaea and Pacific superplumes (e.g. Larson, 1991).

Could the breakup of the Neoproterozoic supercontinent Rodinia (e.g. Moores, 1991; Hoffman, 1991; Dalziel, 1991) also have been caused by a mantle superplume?

Park et al. (1995) first proposed that the breakup of the supercontinent Rodinia could have been triggered by a ca. 780 Ma mantle plume. His main evidence was that radiating mafic dyke swarms along the western margin of Laurentia, together with the plume-related Gairdner dyke swarm in Australia (Zhao et al., 1994), focus at southeastern Australia in a SWEAT configuration (Moores, 1991) (Fig. 1a). However, recent high precision dating has revealed a 827 ± 6 Ma age for the Gairdner dyke swarm, placing it 40 Myr too old to be part of the ca. 780 Ma radiating dyke swarms with which it has been correlated (Wingate et al., 1998).

Li et al. (1999) reported mafic to ultramafic intrusive rocks in central South China of identical age to the Gairdner dyke swarm. They also reported evidence for coeval granitic magmatism, syn-magmatic continental-scale doming, and slightly younger continental rifting. Based on these observations, these authors concluded that the South China Block (SCB) was situated east of Australia right above a mantle plume ca. 825 Ma ago (Fig. 1b), and that this plume triggered the continental rifting during the breakup of Rodinia. However, these authors conceded that the ca. 825 Ma plume was unlikely to have been the only force responsible for the ultimate breakup of Rodinia over 60 Myr later. They speculated that other forces, such as gravity potential created by mantle superswell beneath the supercontinent (Anderson, 1982), and the effects of younger plumes such as the 780 Ma one speculated by Park et al. (1995), were likely also at play. A major shortcoming of this 780 Ma plume model (Park et al., 1995) is the lack of evidence from the continents that

were supposed to be adjacent to western Laurentia at that time (i.e. South China and/or Australia).

In this paper, we report new sensitive high-resolution ion microprobe (SHRIMP) zircon U–Pb ages from South China for magmatic rocks formed during the Neoproterozoic continental rifting (the ca. 780–745 Ma interval in particular), and geochemical evidence for a possible plume origin for this pulse of igneous activity. Based on these results, together with data from other continents, we suggest that plume activities over central and western Rodinia probably lasted over 85 Myr. The evidence for long-lasting, largely synchronous magmatic activity over much of Rodinia, together with geochemical evidence and geological observations, lead to speculation that a mantle superplume was responsible for the breakup of Rodinia.

2. Regional geology and sampling locations

Neoproterozoic anorogenic granitoids and mafic–ultramafic intrusions are widespread around the Yangtze Craton. Their distribution coincides in general with the distribution of Neoproterozoic continental rift systems (e.g. Li, 1991; Li et al., 1999, 2003) (Fig. 2a). The intrusive bodies can be subdivided into two major populations according to their ages relative to the rifting event. The earlier group, generally with an age range of ca. 830–820 Ma, are often overlain unconformably by the rift successions (e.g. Li et al., 1999, 2002a). Granites of the later group, traditionally called the "Chengjiang magmatism", often intrude the rift successions, but in places are unconformably overlain by the equivalent of the late Neoproterozoic Doushantuo Formation (for Neoproterozoic stratigraphy, see Wang and Li, 2003). This group of magmatic intrusions, together with rift volcanics, is therefore called syn-rift magmatism in this paper. Precise age determinations of the syn-rift magmatism, along with geochemical and isotopic analyses of co-magmatic mafic dykes, were the targets of this study.

Out of a total of nine samples dated, seven come from the Kangdian Rift of western South China, and two from the north-eastern end of the Nanhua Rift, eastern South China (Fig. 2). The geology of the two regions and sample localities are described below.

2.1. The Kangdian Rift

The Kangdian Rift is a N–S trending failed Neoproterozoic continental rift in western South China (Fig. 2a) (Li et al., 1999, 2002a; Wang and Li, 2003). The rift was developed on top of a peneplain on strongly deformed, and variably metamorphosed, Mesoproterozoic successions. Radiometric ages for the rift successions (the Suxiong/Kaijianqiao formations) range from ca. 815 ± 12 Ma (Rb–Sr whole rock isochron) at the middle–lower part to 803 ± 12 Ma (SHRIMP zircon U–Pb) at the middle–upper part of the succession (Li et al., 2002a and references herein).

Igneous complexes distribute almost continuously along the Kangdian Rift (Fig. 2b), including granites, granodiorites, tonalites, diorites, gabbros, mafic dykes, and small ultramafic bodies. Some of these igneous complexes, such as the large Shimian granite (SG in Fig. 2b), clearly were formed during the later stages of the rifting because they intrude the rift succession, but are unconformably overlain by the post-rift platform successions (i.e. the equivalent of the late Neoproterozoic Doushantuo Formation). However, igneous complexes that show no intrusive relationships with the Neoproterozoic rift successions have commonly been mapped in the past as part of an Archaean-Paleoproterozoic basement, based on unreliable conventional age determinations (e.g. Sichuan, 1991).

Evidence of magma mingling has been found at numerous outcrops of plutonic bodies along the Dadu River at the northern end of the study region, where ductile gabbroic enclaves are in gradational contact with the surrounding more felsic melt (Fig. 3a). At one locality we observed ductile interaction between mafic dykes and the intruded granitoid (Fig. 3b and c), which we interpret as indicating that the dykes intruded the granitoid when it was still in a semi-solid state. Both these observations suggest that the mafic magma were coeval, and in places co-magmatic, with the granitoids in this region.

Seven geochronological samples were collected from granitoids in the Kamgdian Rift (Fig. 2a and b and Table 1). Some of the associated mafic dykes at the northern end of the region were sampled for geochemical analysis. One dyke which intrudes the Shimian granitoid contains inherited zircon only

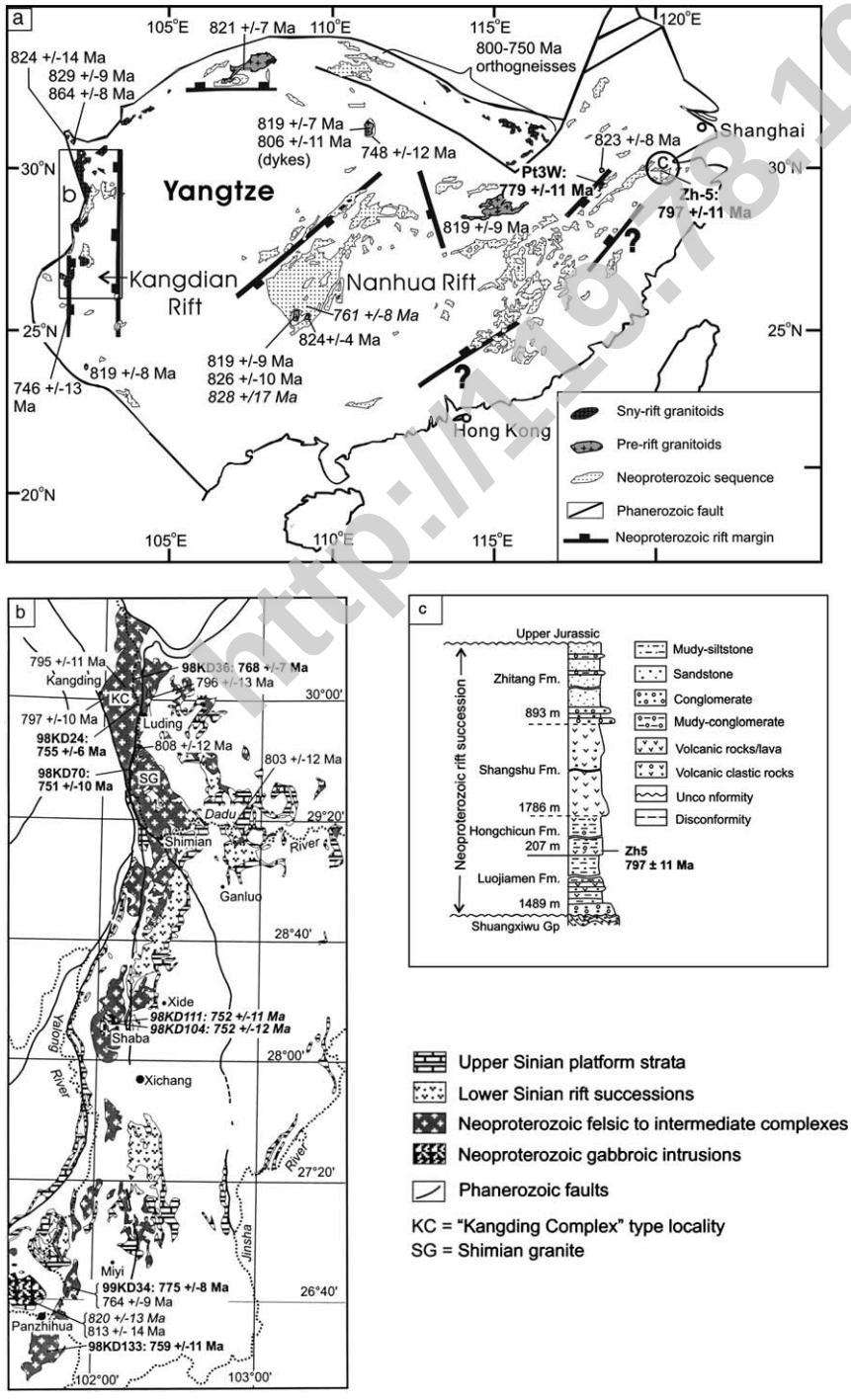

Fig. 2. Neoproterozoic tectonic framework of South China (a) and a more detailed map for northern Kangdian Rift (b). Selected radiometric ages from igneous rocks, as listed in Table 1, are shown. New ages reported in this study are highlighted in bold, and ages from mafic bodies are shown in italic. Neoproterozoic outcrops only are shown for clarity.

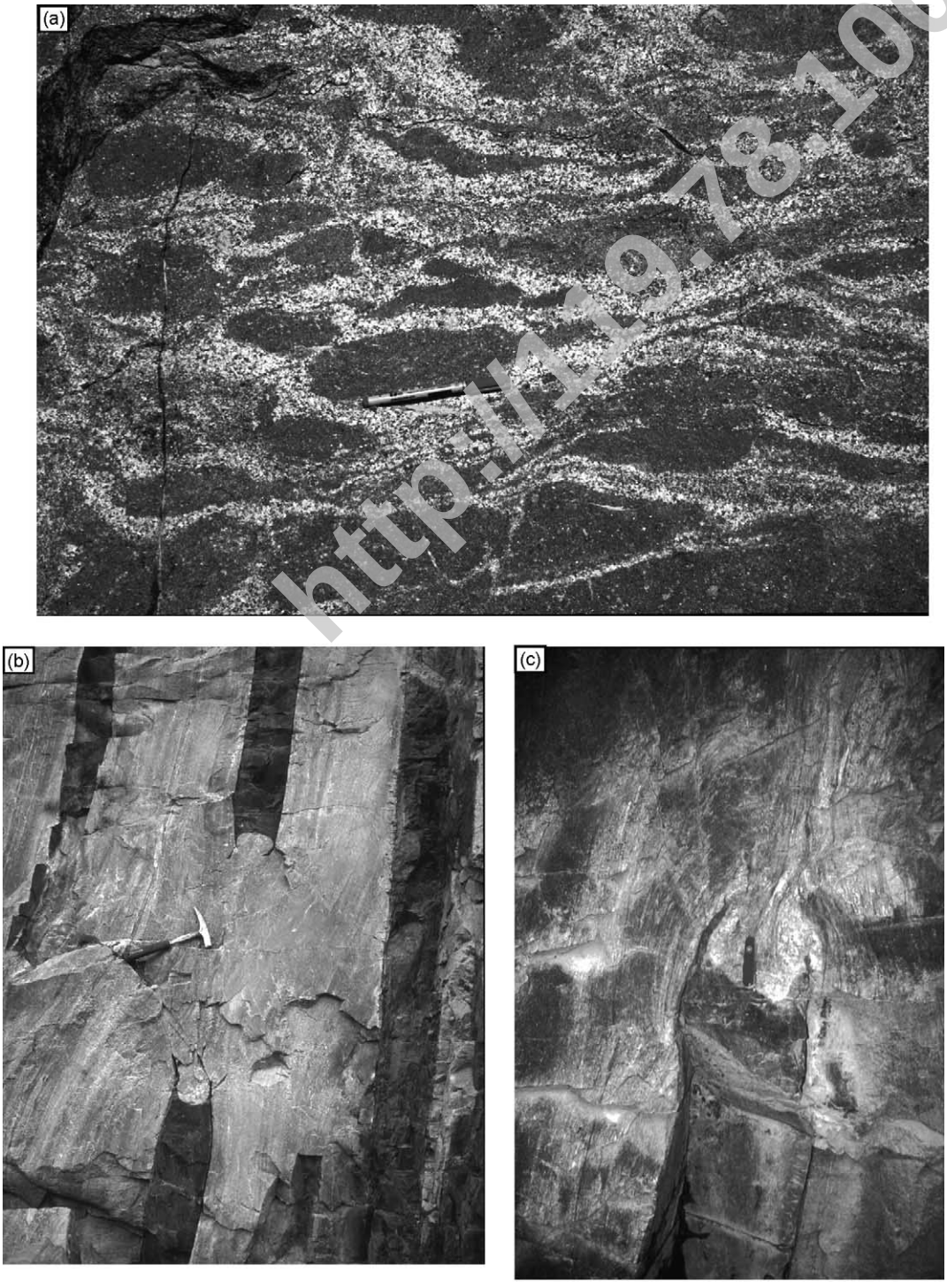

Fig. 3. Photos of magma mingling (a), and ductile interaction between mafic dykes and the intruded granitoid when they both were in semi-solid states (b, c). Photo locations are just north of sampling site 98KD24 in Fig. 2b.

Table 1
List of existing and new age determinations from Neoproterozoic igneous rocks in South China, with data from this study highlighted in bold

Rock (sample) name	Locality[a]		Age (Ma)	+/− (Ma)	Method	References
	Longitude	Latitude				
Granitoids: pre-rift						
Huangling, W Huibei	111°04.040′	30°51.802′	819	7	SHRIMP U–Pb	Ma et al., 1984
Xucun (Tiaoshi body; QnT)	118°20.350′	29°58.617′	823	8	SHRIMP U–Pb	Li et al., 2003
Jiuling, Jiangxi (2KJ1-26-1)	114°58.55′	29°05.25′	819	9	SHRIMP U–Pb	Li et al., 2003
Bendong, Guibei	108.83	25.2	819	9	SHRIMP Pb–Pb	Li, 1999
Sanfang, Guibei	108.84	25.25	826	10	SHRIMP Pb–Pb	Li, 1999
Yuanbaoshan, Guibei	109.2	25.29	824	4	U–Pb lower intercept	Li, 1999
Eshan, Yunnan (98KD154)	120°18.11′	24°05.42′	819	8	SHRIMP U–Pb	Li et al., 2003
Guandaoshan, Yumen, Sichuan	101.86	26.73	857	13	SHRIMP U–Pb	Li et al., 2002b
Danba, Sichuan	102.0	30.8	829	9	U–Pb upper intercept	Roger and Calassou, 1997
Congcai Complex (Gc1), Sichuan	101.83	30.86	824	14	SHRIMP U–Pb	Zhou et al., 2002
Gezong Complex (Gc7), Sichuan	102	30.81	864	8	SHRIMP U–Pb	Zhou et al., 2002
Granitoids: syn-rift						
Kangding Complex (98KD24), Zali, Sichuan	**102°12.756′**	**29°58.033′**	**755**	**6**	**SHRIMP U–Pb**	**This study**
Kangding Complex (98KD36), Sichuan	**102°10.437′**	**30°06.248′**	**768**	**7**	**SHRIMP U–Pb**	**This study**
Kangding Complex (98KD70), Sichuan	**102.17**	**29.54**	**751**	**10**	**SHRIMP U–Pb**	**This study**
Kangding Complex, Kangding (Kd2), Sichuan	102	29.97	797	10	SHRIMP U–Pb	Zhou et al., 2002
Kangding Complex, (Kd11)	102.2	30.04	795	11	SHRIMP U–Pb	Zhou et al., 2002
Kangding Complex, (Kd35)	102.32	30.01	796	13	SHRIMP U–Pb	Zhou et al., 2002
Daxiangling, Sichuan	102.63	29.68	809	22	U–Pb upper intercept	Ma et al., 1989
Datian (98KD133), Sichuan	**101°45.848′**	**26°25.143′**	**759**	**11**	**SHRIMP U–Pb**	**This study**
Miyi (99KD34), Sichuan	**101.86**	**26.73**	**775**	**8**	**SHRIMP U–Pb**	**This study**
Tongde diorite (01KD72), Sichuan	110°33.693′	26°38.581′	813	14	SHRIMP U–Pb	Sinclair, 2001
Miyi (Msta-7), Sichuan	101.9	26.5	764	9	SHRIMP U–Pb	Zhou et al., 2002
Yuanmou (Zb18), Yunnan	101.7	25.7	746	13	SHRIMP U–Pb	Zhou et al., 2002
Shiershan (Pt3W), Anhui	**118°19.625′**	**29°32.162′**	**779**	**11**	**SHRIMP U–Pb**	**This study**
Dabie gneiss	116.4	30.67	773	9.5	U–Pb upper intercept	Rowley et al., 1997
Xiaotian mylonitic granite, Dabie	116.6	31.18	757	0.8	Pb–Pb concodant age	Xue et al., 1997
Orthogneiss (DS236), Dabie	114.66	31.5	779	12	SHRIMP U–Pb	Hacker et al., 2000
Orthogneiss (DS253), Dabie	114.11	31.48	778	7	SHRIMP U–Pb	Hacker et al., 2000
Orthogneiss (DS25), Dabie	115.9	30.97	771	28	TIMS & SHRIMP	Hacker et al., 1998
Tonalite (DS72), Dabie	116.4	30.97	768	31	TIMS & SHRIMP	Hacker et al., 1998
Tuanling tonalite (DS81), Dabie	116.1	30.83	798	33	TIMS & SHRIMP	Hacker et al., 1998
Migmatitic granitoid gneiss (T5), Tongbai	113.41	32.37	746	10	Pb/Pb evaporation	Kröner et al., 1993
Granitoid augengneiss (T7), Tongbai	113.41	32.37	776	8	Pb/Pb evaporation	Kröner et al., 1993
Xiaofeng dykes (99SC1)	111.2	31.1	802	10	SHRIMP U–Pb	Z.X., Li et al., unpublished
Leucogranite (Q89/5), Shaanxi	110.94	33.35	762	0.7	Pb–Pb concodant age	Xue et al., 1996
Gabbros/mafic dykes: pre-rift						
Guibei dykes, Guangxi	108.7	25.2	828	7	SHRIMP Pb–Pb	Li et al., 1999
Tongde gabbro-diorite (99KD36), Sichuan	101°34.138′	26°43.612′	820	13	SHRIMP U–Pb	Sinclair, 2001
Lengji gabbro	102.2	29.8	808	12	SHRIMP U–Pb	X.H., Li et al., unpublished
Shaba gabbro (98KD104), Sichuan	**102.09**	**28.2**	**752**	**12**	**SHRIMP U–Pb**	**This study**
Shaba gabbro (98KD111), Sichuan	**102.08**	**28.21**	**752**	**11**	**SHRIMP U–Pb**	**This study**

Table 1 (*Continued*)

Rock (sample) name	Locality[a]		Age (Ma)	+/− (Ma)	Method	References
	Longitude	Latitude				
Gabbro intruding Sanmenjie Fm, northern Guangxi	109.83	25.68	761	8	Pb–Pb concordant age	Ge et al., 2001
Rift volcanics						
Hongchicun (Zh-5)	**120°07.031′**	**29°55.309′**	**797**	**11**	**SHRIMP U–Pb**	**This study**
Liantuo tuff	111.16	30.85	748	12	SHRIMP U–Pb lower intercept	Ma et al., 1984
Tiechuanshan Fm, Hannan	107°08.03′	32°36.07′	821	7	Pb–Pb concordant age	Ling et al., 2003
Suxiong, Sichuan	102.78	29.33	803	12	SHRIMP U–Pb	Li et al., 2002a

[a] Grids shown in degrees and minutes are from GPS readings; others, shown in decimal point degrees, are estimated from maps.

with ages older than ca. 1100 Ma (sample 98KD75 as reported in Li et al., 2002).

2.2. North-eastern Nanhua Rift

The Neoproterozoic Nanhua Rift is best preserved over the Yangtze side of the rift system, whereas Phanerozoic thrusting towards the Yangtze craton covered part of the rift basin along its NE-trending axis (Wang and Li, 2003) (Fig. 2a). The rift probably branched out to the north-east in a fork-like geometry, in analogy to the branch-off of the Red Sea into the Gulfs of Suez and Aqaba (except that we are dealing with a failed rift here).

Two geochronological samples analysed are from the eastern fork-branch of the rift basin. One sample (Pt3W) is from the Shi'ershan granitoid (Fig. 2a), which is part of a granitic complex that intrude both the Mesoproterozoic Shuangqiaoshan/Shangxi Group metasediments, and the Neoproterozoic rift volcanics (the Shangshu Formation). The complex consists predominantly of leucogranites. Sample Pt3W was collected from the Wutian member at the northern end of the complex. Sample Zh-5 was collected from a fine-grained, intermediate to felsic volcanic unit in the lower Hongchicun Formation, in the lower part of the Neoproterozoic rift succession (Fig. 2c; Wang and Li, 2003). This formation consists predominantly of immature clastic rocks deposited in shelf to near-shore environments, with minor volcanic intervals at both the bottom and top parts of the formation. An age for the Hongchicun Formation will constrain on the timing of volcanic activity during the early rifting stage.

3. New SHRIMP geochronological results

3.1. Analytical method

Zircon concentrates from all samples were mounted with zircon standard CZ3 (550 ppm U, $^{206}Pb^*/^{238}U = 0.0914$) in the University of Western Australia mineral separation laboratory. Both optical photomicrographs and backscattered electron or cathodoluminescence (CL) images were taken as a guide to isotopic analytical spot selection. U–Pb isotopic analyses were done using the SHRIMP-II ion microprobe at Curtin University of Technology, using standard operating conditions (7-scan duty cycle, 2 nA primary O_2^- beam, 25 μm analytical spot size, mass resolution ca. 5000). The common Pb component was estimated from ^{204}Pb counts, assuming a typical terrestrial common Pb composition for the indicated age (Stacey and Kramers, 1975). Accumulated data for the standard CZ3 were used to correct for Pb/U elemental fractionation. Data reduction was carried out using the KRILL and PLONK software programs written by P.D.K. and David Nelson, respectively. Measured isotopic ratios and calculated ages for individual spot analyses are given in Table 2, and concordia plots of results are shown in Figs. 4 and 5. Ages are quoted in the text with uncertainties at 95% confidence.

3.2. New ages from the northern Kangdian Rift

All samples analysed show no or only a weak foliation. Sample 98KD36 is from a diorite body about 4 km north of the village Guzan, traditionally

Table 2
SHRIMP zircon U–Pb data for selected magmatic rocks from South China

Spot	U (ppm)	Th (ppm)	Th/U	%com ^{206}Pb	^{207}Pb/^{206}Pb	±1σ	^{206}Pb/^{238}U	±1σ	^{207}Pb/^{235}U	±1σ	^{206}Pb/^{238}U	
											AGE	±1σ
98KD36												
9	91	124	1.37	0.56	0.0648	0.0028	0.1285	0.0015	1.148	0.053	780	8
2	48	50	1.05	1.28	0.0643	0.0049	0.1279	0.0019	1.133	0.090	776	11
7	119	174	1.46	0.31	0.0650	0.0022	0.1280	0.0013	1.147	0.041	776	7
1	93	131	1.42	0.73	0.0639	0.0029	0.1274	0.0014	1.122	0.055	773	8
4	48	45	0.93	0.96	0.0644	0.0059	0.1274	0.0019	1.131	0.107	773	11
5	64	122	1.90	0.75	0.0672	0.0037	0.1265	0.0017	1.173	0.068	768	10
3	46	52	1.13	2.10	0.0589	0.0052	0.1263	0.0019	1.026	0.094	767	11
8	73	89	1.22	0.76	0.0656	0.0037	0.1262	0.0016	1.141	0.068	766	9
10	100	128	1.28	1.06	0.0630	0.0027	0.1261	0.0014	1.095	0.050	765	8
14	92	125	1.35	1.26	0.0631	0.0031	0.1256	0.0014	1.093	0.057	763	8
13	40	45	1.12	2.11	0.0652	0.0066	0.1253	0.0021	1.127	0.118	761	12
6	45	47	1.04	0.87	0.0690	0.0056	0.1249	0.0019	1.189	0.101	759	11
11	68	76	1.13	1.83	0.0618	0.0050	0.1248	0.0017	1.063	0.089	758	10
12	140	233	1.67	0.96	0.0622	0.0020	0.1245	0.0013	1.067	0.038	756	8
15	279	50	0.18	0.25	0.0655	0.0015	0.1218	0.0011	1.099	0.027	741	6
98KD24												
2	514	1082	2.11	0.54	0.0641	0.0009	0.1276	0.0009	1.128	0.018	774	5
7	412	879	2.13	0.23	0.0651	0.0010	0.1265	0.0010	1.135	0.020	768	5
8	166	243	1.46	0.52	0.0653	0.0017	0.1255	0.0012	1.130	0.033	762	7
3	193	227	1.18	0.54	0.0651	0.0021	0.1250	0.0011	1.121	0.039	759	6
1	59	82	1.39	1.88	0.0645	0.0044	0.1248	0.0017	1.111	0.079	758	10
14	304	431	1.42	0.69	0.0639	0.0013	0.1240	0.0010	1.092	0.026	754	6
13	464	640	1.38	0.39	0.0633	0.0009	0.1238	0.0009	1.081	0.018	753	5
4	411	1025	2.49	0.32	0.0653	0.0009	0.1237	0.0010	1.114	0.018	752	6
9	461	725	1.57	0.22	0.0642	0.0008	0.1237	0.0009	1.096	0.016	752	5
5	166	232	1.40	0.93	0.0644	0.0020	0.1232	0.0011	1.093	0.037	749	7
12	91	162	1.78	1.73	0.0616	0.0038	0.1228	0.0014	1.042	0.067	746	8
6	131	180	1.38	1.16	0.0621	0.0026	0.1217	0.0012	1.042	0.046	741	7
10	58	69	1.20	5.84	0.0602	0.0079	0.1215	0.0018	1.009	0.136	739	11
15	163	223	1.37	1.84	0.0599	0.0032	0.1210	0.0014	1.000	0.056	736	8
11	306	562	1.84	0.54	0.0633	0.0013	0.1201	0.0010	1.048	0.024	731	6
98KD70												
1	714	1484	2.08	0.21	0.0652	0.0009	0.1281	0.0016	1.152	0.022	777	9
10	305	262	0.86	0.49	0.0620	0.0011	0.1264	0.0016	1.080	0.025	767	9
4	288	327	1.13	0.37	0.0640	0.0012	0.1238	0.0016	1.092	0.026	752	9
11	123	86	0.70	0.39	0.0633	0.0022	0.1238	0.0018	1.081	0.042	752	10
13	384	376	0.98	0.36	0.0633	0.0011	0.1231	0.0016	1.074	0.024	748	9
8	421	537	1.27	0.22	0.0640	0.0008	0.1229	0.0015	1.084	0.021	747	9
2	96	71	0.74	0.95	0.0674	0.0030	0.1226	0.0021	1.140	0.056	745	12
3	262	295	1.13	0.34	0.0641	0.0012	0.1225	0.0016	1.082	0.026	745	9
12	903	1405	1.56	0.28	0.0641	0.0006	0.1225	0.0016	1.083	0.018	745	9
5	223	224	1.00	0.37	0.0644	0.0014	0.1221	0.0016	1.085	0.029	743	9
6	493	472	0.96	0.24	0.0637	0.0007	0.1221	0.0015	1.072	0.019	743	9
7	170	143	0.85	0.57	0.0626	0.0019	0.1217	0.0016	1.051	0.036	740	9
14	282	474	1.68	0.41	0.0628	0.0016	0.1132	0.0015	0.981	0.029	692	9
9	320	508	1.59	0.28	0.0636	0.0010	0.1098	0.0015	0.963	0.021	672	8
98KD104												
8	63	75	1.18	2.38	0.0637	0.0053	0.1287	0.0026	1.130	0.100	781	15
6	32	20	0.62	1.71	0.0765	0.0093	0.1268	0.0031	1.336	0.170	769	18

Table 2 (*Continued*)

Spot	U (ppm)	Th (ppm)	Th/U	%com ^{206}Pb	^{207}Pb/^{206}Pb	±1σ	^{206}Pb/^{238}U	±1σ	^{207}Pb/^{235}U	±1σ	^{206}Pb/^{238}U AGE	±1σ
14	90	80	0.88	1.19	0.0648	0.0042	0.1265	0.0023	1.130	0.079	768	13
11	199	308	1.55	0.44	0.0651	0.0018	0.1261	0.0021	1.132	0.039	766	12
7	105	147	1.40	0.40	0.0674	0.0026	0.1260	0.0022	1.171	0.052	765	13
10	147	170	1.16	0.48	0.0641	0.0020	0.1247	0.0021	1.101	0.041	758	12
4	94	125	1.33	1.82	0.0617	0.0045	0.1242	0.0024	1.056	0.083	754	14
2	59	42	0.72	2.16	0.0634	0.0051	0.1242	0.0021	1.085	0.092	754	12
13	47	40	0.86	2.80	0.0551	0.0071	0.1230	0.0027	0.934	0.124	748	15
3	209	354	1.69	0.38	0.0664	0.0017	0.1228	0.0020	1.124	0.036	746	12
15	77	75	0.97	0.78	0.0651	0.0036	0.1225	0.0023	1.099	0.067	745	13
1	156	229	1.47	1.41	0.0653	0.0025	0.1222	0.0017	1.100	0.047	743	10
5	34	21	0.63	5.66	0.0522	0.0120	0.1186	0.0031	0.854	0.201	723	18
9	106	149	1.40	1.64	0.0566	0.0038	0.1178	0.0023	0.919	0.067	718	13
12	106	166	1.56	2.53	0.0510	0.0097	0.0954	0.0024	0.670	0.131	588	14
98KD111												
10	51	52	1.01	1.59	0.0609	0.0056	0.1273	0.0027	1.068	0.104	772	15
11	75	91	1.20	0.70	0.0675	0.0045	0.1267	0.0024	1.180	0.085	769	14
6	89	76	0.84	2.60	0.0612	0.0046	0.1263	0.0024	1.065	0.086	767	14
1	81	80	0.98	2.31	0.0593	0.0047	0.1260	0.0024	1.030	0.086	765	14
14	60	45	0.75	2.10	0.0706	0.0068	0.1252	0.0026	1.218	0.123	761	15
3	126	83	0.66	0.84	0.0604	0.0026	0.1252	0.0022	1.042	0.050	760	13
12	85	65	0.76	1.85	0.0595	0.0041	0.1249	0.0023	1.026	0.075	759	13
15	87	85	0.98	0.91	0.0680	0.0034	0.1243	0.0023	1.166	0.064	755	13
2	57	56	0.97	2.05	0.0620	0.0054	0.1234	0.0025	1.055	0.098	750	14
13	83	88	1.05	1.89	0.0613	0.0044	0.1229	0.0023	1.040	0.080	747	13
4	74	74	1.00	2.30	0.0588	0.0046	0.1213	0.0023	0.984	0.081	738	13
9	69	55	0.81	2.30	0.0593	0.0053	0.1213	0.0024	0.991	0.094	738	14
5	64	70	1.09	1.06	0.0653	0.0046	0.1202	0.0024	1.082	0.081	732	14
8	101	108	1.07	1.09	0.0615	0.0033	0.1197	0.0022	1.015	0.060	729	13
7	133	156	1.18	1.64	0.0710	0.0165	0.1101	0.0038	1.078	0.259	674	22
99KD34												
3	114	105	0.92	0.53	0.0639	0.0027	0.1303	0.0017	1.148	0.052	789	10
2	152	131	0.86	0.19	0.0659	0.0020	0.1299	0.0017	1.180	0.041	787	10
8	121	161	1.33	1.66	0.0610	0.0037	0.1299	0.0018	1.092	0.070	787	10
10	74	64	0.87	0.27	0.0669	0.0039	0.1294	0.0020	1.192	0.074	784	11
4	132	198	1.50	0.60	0.0640	0.0028	0.1292	0.0020	1.139	0.054	783	11
1b	73	58	0.80	0.00	0.0701	0.0016	0.1289	0.0019	1.247	0.035	782	11
5	107	135	1.26	0.25	0.0681	0.0029	0.1290	0.0021	1.211	0.057	782	12
14	129	132	1.02	0.43	0.0636	0.0021	0.1288	0.0016	1.130	0.041	781	9
15	82	55	0.67	0.32	0.0637	0.0031	0.1286	0.0023	1.130	0.062	780	13
6	118	147	1.25	0.72	0.0635	0.0033	0.1282	0.0017	1.122	0.062	778	10
9	210	272	1.29	0.37	0.0618	0.0019	0.1280	0.0016	1.090	0.038	776	9
16	124	104	0.84	0.54	0.0638	0.0024	0.1278	0.0016	1.124	0.046	775	9
12	52	47	0.90	0.64	0.0642	0.0070	0.1270	0.0023	1.125	0.127	771	13
13	186	141	0.75	0.08	0.0672	0.0017	0.1259	0.0015	1.167	0.033	764	9
1a	114	165	1.45	1.45	0.0625	0.0042	0.1254	0.0017	1.080	0.076	762	10
7	124	170	1.37	0.05	0.0690	0.0024	0.1253	0.0016	1.192	0.046	761	9
11	172	151	0.88	0.26	0.0638	0.0018	0.1231	0.0015	1.083	0.034	748	9
98KD133												
10	88	66	0.75	1.29	0.0618	0.0037	0.1286	0.0024	1.095	0.071	780	14
2	76	63	0.83	2.11	0.0639	0.0047	0.1274	0.0024	1.123	0.087	773	14

Table 2 (*Continued*)

Spot	U (ppm)	Th (ppm)	Th/U	%com ^{206}Pb	^{207}Pb/^{206}Pb	±1σ	^{206}Pb/^{238}U	±1σ	^{207}Pb/^{235}U	±1σ	^{206}Pb/^{238}U AGE	±1σ
4	166	174	1.05	0.83	0.0647	0.0020	0.1272	0.0021	1.135	0.042	772	12
7	54	37	0.68	5.13	0.0535	0.0084	0.1270	0.0029	0.938	0.151	771	17
14	75	60	0.80	2.19	0.0652	0.0050	0.1271	0.0024	1.143	0.094	771	14
8	111	93	0.84	1.05	0.0621	0.0025	0.1260	0.0022	1.079	0.050	765	13
6	64	55	0.87	1.27	0.0673	0.0053	0.1245	0.0025	1.156	0.097	757	14
12	98	77	0.79	1.84	0.0633	0.0039	0.1244	0.0023	1.086	0.072	756	13
15	385	502	1.30	0.30	0.0655	0.0010	0.1243	0.0020	1.124	0.027	755	11
3	97	70	0.72	1.04	0.0662	0.0036	0.1240	0.0023	1.131	0.068	753	13
11	76	62	0.81	2.88	0.0577	0.0056	0.1239	0.0024	0.986	0.100	753	14
1	118	107	0.90	1.50	0.0669	0.0031	0.1228	0.0022	1.132	0.059	746	12
5	145	158	1.09	0.90	0.0625	0.0025	0.1204	0.0021	1.038	0.048	733	12
9	72	58	0.81	2.57	0.0560	0.0065	0.1107	0.0028	0.854	0.104	677	16
13	95	76	0.81	1.89	0.0668	0.0129	0.1047	0.0033	0.964	0.193	642	19
Pt3W												
6	465	165	0.36	0.00	0.0670	0.0006	0.1417	0.0025	1.308	0.027	854	14
11	224	163	0.73	0.00	0.0667	0.0008	0.1311	0.0024	1.206	0.029	794	14
14	199	108	0.54	0.03	0.0660	0.0016	0.1310	0.0024	1.192	0.038	794	14
4	309	183	0.59	0.09	0.0657	0.0012	0.1306	0.0023	1.182	0.032	791	13
3	198	112	0.57	0.03	0.0665	0.0018	0.1301	0.0024	1.193	0.041	788	14
8	243	156	0.64	0.10	0.0648	0.0014	0.1299	0.0023	1.161	0.035	788	13
10	264	143	0.54	0.08	0.0658	0.0012	0.1285	0.0025	1.165	0.032	779	14
2	152	81	0.53	0.12	0.0662	0.0014	0.1280	0.0024	1.168	0.035	776	14
7	276	186	0.68	0.04	0.0643	0.0011	0.1280	0.0025	1.135	0.032	776	14
12	160	80	0.50	0.35	0.0614	0.0016	0.1279	0.0024	1.082	0.037	776	14
1	202	104	0.51	0.00	0.0652	0.0013	0.1276	0.0024	1.148	0.033	774	14
5	92	44	0.47	0.23	0.0618	0.0035	0.1273	0.0027	1.084	0.068	772	15
15	335	248	0.74	0.03	0.0664	0.0011	0.1272	0.0023	1.165	0.030	772	13
9	107	57	0.54	0.04	0.0653	0.0027	0.1266	0.0025	1.140	0.054	768	14
13	180	116	0.64	0.04	0.0655	0.0016	0.1234	0.0023	1.114	0.037	750	13
98 Zh-5												
8	85	44	0.52	3.68	0.0653	0.0059	0.1491	0.0033	1.343	0.128	896	18
18	83	46	0.56	1.84	0.0627	0.0043	0.1360	0.0029	1.176	0.087	822	16
20	76	41	0.54	1.78	0.0644	0.0040	0.1350	0.0029	1.199	0.082	816	16
19	161	123	0.76	0.90	0.0666	0.0021	0.1344	0.0026	1.235	0.049	813	15
6	107	64	0.60	1.63	0.0631	0.0038	0.1344	0.0028	1.169	0.078	813	16
13	73	36	0.50	2.72	0.0698	0.0058	0.1340	0.0030	1.290	0.115	811	17
16	85	48	0.56	2.03	0.0665	0.0040	0.1336	0.0028	1.225	0.082	808	16
7	60	26	0.43	2.23	0.0660	0.0062	0.1330	0.0031	1.210	0.121	805	18
5	105	61	0.58	1.53	0.0646	0.0037	0.1329	0.0028	1.183	0.075	804	16
11	68	32	0.47	2.47	0.0692	0.0059	0.1322	0.0030	1.261	0.114	801	17
14	66	30	0.46	1.82	0.0678	0.0049	0.1322	0.0029	1.236	0.097	800	17
15	47	20	0.42	2.58	0.0674	0.0073	0.1320	0.0031	1.226	0.140	799	18
4	112	67	0.60	1.69	0.0639	0.0035	0.1320	0.0028	1.162	0.072	799	16
12	79	39	0.50	2.80	0.0687	0.0054	0.1314	0.0029	1.244	0.106	796	17
2	86	44	0.51	2.64	0.0672	0.0053	0.1286	0.0029	1.192	0.101	780	16
9	70	34	0.48	3.84	0.0538	0.0065	0.1286	0.0030	0.953	0.120	780	17
3	74	40	0.54	3.76	0.0639	0.0065	0.1281	0.0029	1.129	0.121	777	17
10	77	41	0.53	2.99	0.0580	0.0058	0.1280	0.0029	1.023	0.107	776	17
1	82	47	0.57	2.49	0.0594	0.0055	0.1271	0.0028	1.041	0.102	771	16
17	51	24	0.47	2.76	0.0575	0.0072	0.1268	0.0030	1.006	0.131	769	17

Note: %com ^{206}Pb is the percentage of common ^{206}Pb, estimated from the measured ^{204}Pb/^{206}Pb ratio.

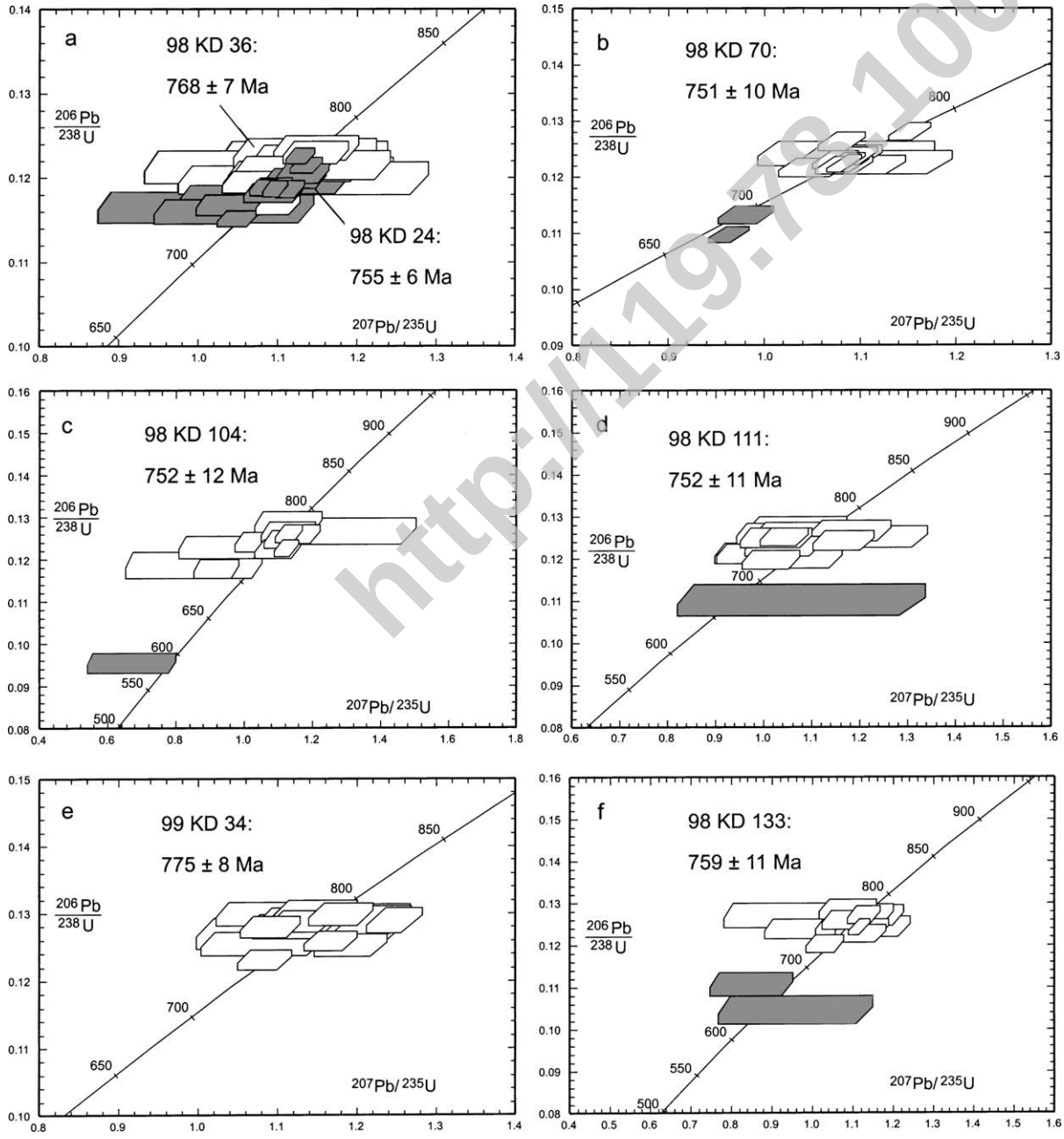

Fig. 4. Concordia plots of samples from the Kangdian Rift (see list in Table 1).

mapped as part of the type Archaean-Paleoproterozoic "Kangding Complex" (Fig. 2b). Zircon grains from this sample are euhedral in shape, with little or no internal zonation visible under CL. U–Pb analyses of 15 grains were undertaken. Fourteen analyses form a simple concordant population with a mean $^{206}Pb/^{238}U$ age of 768 ± 7 Ma (Fig. 4a). Analysis #15 was slightly younger.

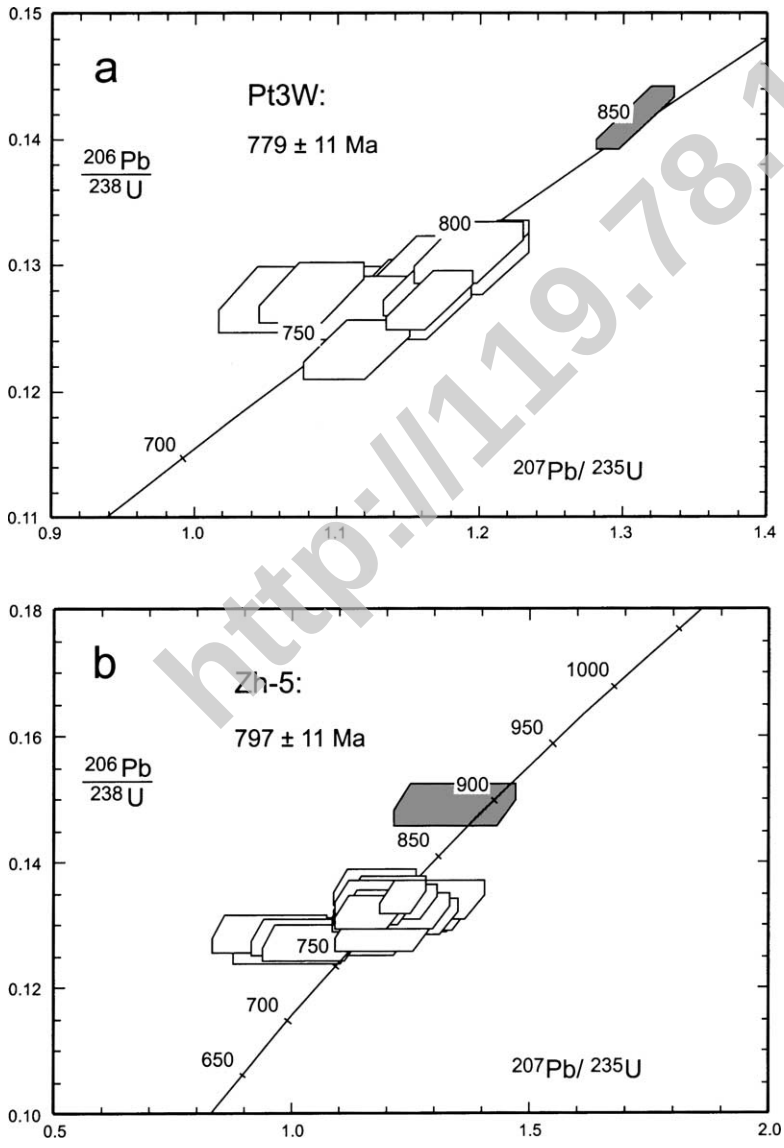

Fig. 5. Concordia plots of samples from the north-eastern Nanhua Rift: (a) sample Pt3W from the Shi'ershan granite, and (b) sample Zh-5 from a intermediate to felsic volcanic unit in lower Hongchicun Formation (Fig. 2, and Table 1).

Sample 98KD24 is from a granodiorite member of the "Kangding Complex" which locally contains abundant mafic enclaves, about 14 km south of 98KD36 (Fig. 2b). Zircon grains from this sample are typical euhedral magmatic grains showing fine internal zonation in CL images. Out of the 15 analyses undertaken on as many grains, ten combine to give a mean $^{206}Pb/^{238}U$ age of 755 ± 6 Ma (Fig. 4a), with four analyses yielding slightly younger ages and one slightly older. The apparent scatter in $^{206}Pb/^{238}U$ ages is likely due to a slight underestimation of analytical uncertainty, and/or to Pb loss. The calculated age is slightly younger than that calculated for 98KD36, which was analysed in the same session.

Sample 98KD70 is from a granitic body at the southern tip of the type "Kangding Complex"

(Fig. 2b). The zircon crystals are euhedral with CL images showing clear oscillatory growth zonation. Out of a total of 14 grains analysed, 12 form a concordant group with a mean $^{206}Pb/^{238}U$ age of 751 ± 10 Ma, whilst two yielded significantly younger ages due to partial Pb loss (Fig. 4b). This result is consistent within error with the age for 98KD24. All three new ages from the type locality of the "Kangding Complex" are 30–40 my younger than the SHRIMP zircon U–Pb ages reported by Zhou et al. (2002) from different members of the complex. It is thus likely that the "Kangding Complex" type locality consists of granitic intrusions of different ages.

Samples 98KD104 and 98KD111 are both from the Shaba intrusive complex, west of Xide (Fig. 2b) which was mapped as part of the "Kangding Complex", with the central part of the complex mapped as "granulite facies gneisses" (Sichuan, 1991). However, our field and laboratory examination revealed that these rocks are diorites to gabbros. Both samples 98KD104 and 98KD111 are from gabbroic members of the complex.

Zircon grains in 98KD104 are clear, euhedral prismatic grains with simple internal growth zonation, whereas zircon grains in sample 98KD111 are mostly anhedral grains with internal zonation truncated at the grain margins, suggesting partial resorption of originally larger grains. SHRIMP analyses of 14 grains from sample 98KD104 form a simple concordant population with a mean $^{206}Pb/^{238}U$ age of 752 ± 12 Ma (Fig. 4c). One additional analysis (#12) yielded a significantly younger $^{206}Pb/^{238}U$ age of ca. 590 Ma, most likely because of Pb loss. For sample 98KD111, with the exception of one analysis showing partial Pb loss (#7), the remainder 14 SHRIMP analyses data for this sample give to a mean $^{206}Pb/^{238}U$ age of 752 ± 11 Ma (Fig. 4d).

Sample 99KD34 is from a weakly foliated quartz diorite about 20 km north-east of Panzhihua (Fig. 2b), previously mapped as part of the Archaean-Paleoproterozoic "Kangding Complex" (Sichuan, 1991). Zircon grains in this sample are mostly euhedral in shape, with regular internal growth zonation. A mean $^{206}Pb/^{238}U$ age of 775 ± 8 Ma was calculated from 17 spot analyses of individual grains (Fig. 4e).

Sample 98KD133 is from a granodiorite south of Panzhihua (Fig. 2b) that shows no visible foliation, but again was previously mistaken as part of the Archaean-Paleoproterozoic "Kangding Complex" (Sichuan, 1991). Zircon grains in this sample have simple prismatic igneous shapes and internal zonation. The combined $^{206}Pb/^{238}U$ age from 13 spot analyses was 759 ± 11 Ma, with two additional analyses yielding younger results (Fig. 4f).

3.3. New ages from north-eastern Nanhua Rift

Sample Pt3W from the Shi'ershan granitoid yielded an euhedral population of zircon grains. Apart from one analysis of older, inherited grain ($^{206}Pb/^{238}U$ age ca. 854 Ma), SHRIMP analyses of 14 grains combine to a mean $^{206}Pb/^{238}U$ age of 779 ± 11 Ma for the magmatism (Fig. 5a). This age is identical to that of sample 99KD34 from the Kangdian Rift.

Zircon grains from sample Zh-5 have simple prismatic crystal shapes, with magmatic internal zonation revealed by CL imaging. With the exception of one significantly older analysis (#8), the SHRIMP data form a concordant group ($N = 19$) giving a mean $^{206}Pb/^{238}U$ age of 797 ± 11 Ma (Fig. 5b).

4. Pulses of Neoproterozoic magmatic rocks in South China, accompanied by continental rift and rapid cruatal unroofing

Fig. 6 plots the distribution of known igneous rocks in South China for the 880–720 Ma interval, including the new data reported in this study. Sources and descriptions of the data are listed in Table 1.

Fig. 6a highlights the existence of two major episodes of intrusions/eruptions of felsic to intermediate rocks: one between 830 and 795 Ma, and the other between 780 and 745 Ma. There is an apparent gap of 10–15 Ma between the two episodes, and there are sub-peaks within each episode. In addition, there is a minor peak at around 860 Ma, which occurs as granitoids in western South China (Table 1). This age group also appeared in an inherited zircon grain in the Shi'ershan granitoid (Fig. 5a; excluded from the histogram) in eastern South China.

Fig. 6b plots the temporal distribution of mafic rocks in South China. Given that mafic rocks are normally difficult to date, this figure is likely an under-representation of the amount of mafic to ultramafic rocks in South China in comparison with the number of data from the more felsic rocks. The figure

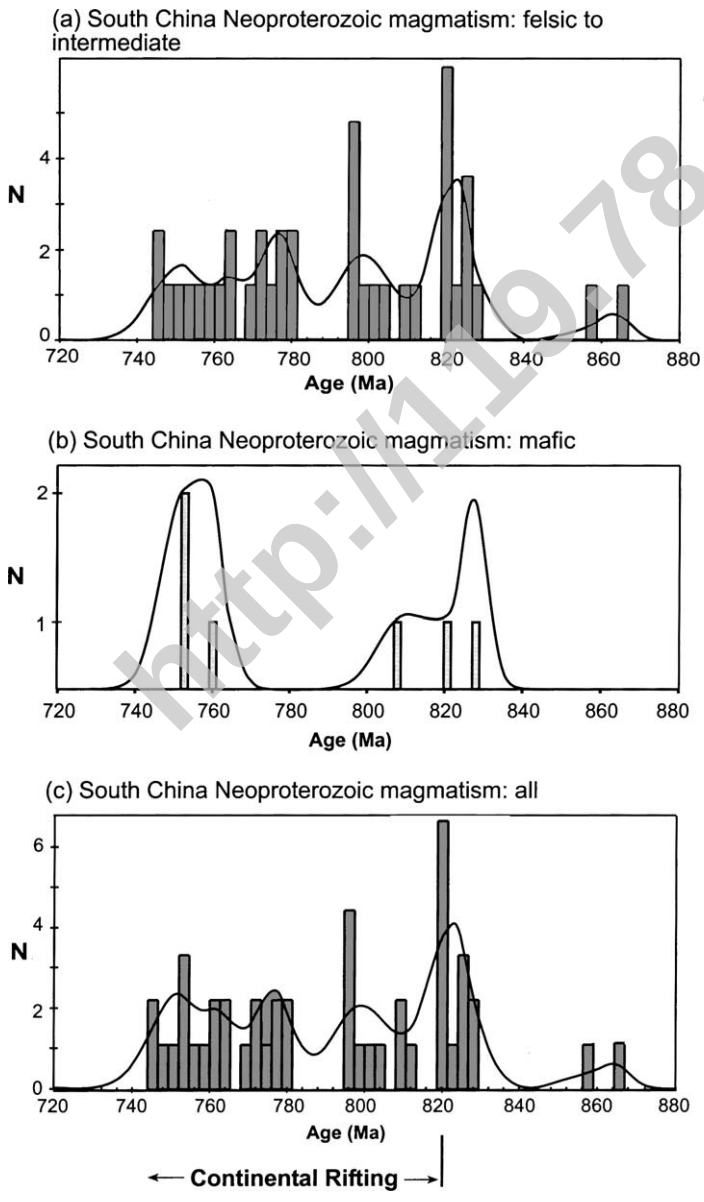

Fig. 6. Age distribution of igneous rocks in South China between 880 and 720 Ma: (a) felsic to intermediate rocks only, (b) mafic rocks only, and (c) all igneous rocks. Plots generated using ISOPLOT developed by Ludwig (2001).

nonetheless indicates the existence of the same two episodes of igneous activity as shown by the felsic to intermediate rocks in Fig. 6a. This suggests that both episodes of magmatic activities were bimodal. The presence of intermediate rocks could be the result of magma mixing.

Fig. 6c plots all magmatic ages listed in Table 1. A salient feature is that the 830–795 Ma episode of magmatism peaked at the starting point of continental rifting at ca. 820 Ma (e.g. Li et al., 1999; Wang and Li, 2003). Given the bimodal nature of the magmatism, and the close temporal and spatial associations of the

pre-rift magmatism (Li et al., 2003) with the continental rifting (Figs. 2 and 6c), it is most likely that both the pre-rift magmatism (the ca. 830–820 Ma magmatism, and possibly the ca. 860 Ma minor episode as well) and the syn-rift magmatism (820–745 Ma) occurred in an extensional regime. This interpretation is in contrast with the convergent settings suggested by some early workers for both the pre-rift magmatism (e.g. Li, 1999) and the syn-rift magmatism (e.g. Zhou et al., 2002).

Furthermore, both episodes of magmatism were accompanied by rapid lithospheric doming. The early phase of doming is demonstrated by the widespread depositional contact between the ca. 820 Ma pre-rift granites and similar-aged rift volcaniclastic successions (Li et al., 1999, 2003). Syn-rift doming is demonstrated by the deposition of the post-rift clastic deposits along the Kangdian rift over either the ca. 810 Ma Shimian granite (also called Daxiangling granite), or the 800–750 Ma granitoid intrusions near Kangding. If the 830–795 Ma episode of magmatism was the result of a ca. 825 Ma mantle plume, as suggested by Li et al. (1999) and Li et al. (2003), could the 780–745 Ma episode be related to the ca. 780 Ma plume event in western Laurentia, as speculated by Park et al. (1995)?

5. Geochemical and Nd isotopic analyses of mafic dykes from the Kangding Rift support a mantle plume origin

We analysed the major and trace elements and Nd isotope composition of some mafic dykes in the Kangdian rift that are co-magmatic with the 760–740 Ma granodiorites in western South China (Figs. 2 and 3; Table 3), in order to examine whether they could have been derived from a mantle plume. Major elements were determined using a Philips PW 1400 X-ray fluorescence spectrometer (XRF) at the School of Earth and Geographical Sciences, the University of Western Australia. Trace elements were determined using a Perkin-Elmer Sciex ELAN 6000 ICP-MS at the Guangzhou Institute of Geochemistry. Nd isotopic compositions were determined using a Micromass Isoprobe multi-collector (MC-ICPMS) operated in static mode at the Guangzhou Institute of Geochemistry. Analytical procedures were the same

Table 3
Geochemical and Nd isotopic data for representative mafic dyke samples

Sample	01KD09	01KD11	01KD15A	01KD16
Location	30°21.5′N 102°07.9′E	30°21.5′N 102°07.9′E	30°19.0′N 102°09.9′E	30°19.0′N 102°09.9′E
Dyke thickness	~100 cm	~30 cm	~25 cm (Fig. 3c)	~20 cm
Major elements (%)				
SiO_2	48.00	46.36	49.12	49.16
TiO_2	1.45	1.51	0.96	1.46
Al_2O_3	16.95	16.59	19.42	16.46
$Fe_2O_3{}^T$	12.39	14.12	11.08	12.06
MnO	0.21	0.18	0.19	0.20
MgO	6.68	5.47	5.27	6.37
CaO	9.79	7.71	8.08	9.28
Na_2O	1.47	0.09	1.20	1.69
K_2O	2.90	7.87	4.61	3.25
P_2O_5	0.30	0.24	0.19	0.26
Total	100.14	100.14	100.12	100.19
Mg#	0.56	0.48	0.53	0.55
LOI	2.59	7.83	2.43	2.21
Trace elements (ppm)				
Sc	80.4	72.7	87.6	83.5
V	214	194	224	230
Cr	134	81.9	81.5	124
Co	33.5	29.3	24.9	28.8
Ni	111	19.4	44.0	87.1
Ga	17.1	19.8	19.3	18.2
Rb	77.1	222	258	94.5
Sr	227	70.0	289	205
Y	27.1	27.3	16.2	22.4
Zr	128	127	103	148
Nb	3.36	9.92	1.45	3.72
Ba	737	1381	321	346
La	10.3	12.7	9.1	10.9
Ce	24.4	27.3	20.8	25.3
Pr	3.50	3.68	2.90	3.64
Nd	17.0	16.0	13.2	17.0
Sm	4.19	3.59	3.06	3.93
Eu	1.66	0.79	1.17	1.65
Gd	4.92	4.09	3.22	4.27
Tb	0.85	0.78	0.55	0.79
Dy	5.27	4.94	3.23	4.45
Ho	1.11	1.08	0.67	0.96
Er	3.36	3.50	2.03	2.82
Tm	0.58	0.68	0.37	0.49
Yb	3.15	3.70	2.03	2.71
Lu	0.48	0.59	0.32	0.43
Hf	3.10	3.43	2.41	3.46
Ta	0.23	0.70	0.10	0.27
Th	1.07	1.89	0.76	1.65
U	0.56	0.79	0.57	0.59

Table 3 (*Continued*)

Sample	01KD09	01KD11	01KD15A	01KD16
$^{143}Nd/^{144}Nd$	0.512556	0.512506	0.512399	0.512496
Error ($2\sigma_m$)	0.000011	0.000011	0.000010	0.000009
$\varepsilon Nd(T)$	3.1	3.4	0.9	2.8

Mg# = $Mg/(Mg+Fe^{2+})$, assuming $Fe_2O_3/(FeO+Fe_2O_3) = 0.20$. Total iron as Fe_2O_3. T = 760 Ma, emplacement age estimated from the co-magmatic granitoids.

as described in a separate paper by Li et al. (2003), and the data are presented in Table 3.

All samples experienced various degrees of alteration as shown by their high LOI values (2.2–7.8%). Na and K are mobile and their contents are susceptible to changes during alteration; they are thus unsuitable for classification of rock types. According to the essentially immobile elements, such as the high-field-strength elements (HFSE) and REE, these mafic dykes are generally of tholeiitic composition, with low Nb/Y ratios (0.09–0.35), moderate TiO_2 contents (1–1.5%) and relatively flat REE patterns (Fig. 7a). The very low Sr content (70 ppm) and a clear Eu negative anomaly in sample 01KD11 are attributed to severe alteration (LOI = 7.8%).

In a MORB-normalised spidergram (Fig. 7b; Pearce, 1982), the tholeiitic mafic dykes display significant variations in the abundances of Sr, K, Rb and Ba, likely due to their mobility during subsequent alteration. Apart from Nb–Ta, the immobile trace elements show a general increase in normalised abundance from Yb to Th. The enrichment in Th, light REE and HSFE relative to MORB, and the high Zr/Y (4.7–6.6) and Zr/Sm (30–37) ratios, resemble those of intra-plate tholeiites ($Zr/Y > 3.5$, $Zr/Sm \approx 30$), but are significantly different from those of island arc tholeiites ($Zr/Y < 3.5$, $Zr/Sm < 20$) (Pearce and Norry, 1979; Wilson, 1989). Thus, clear Nb–Ta depletions and relatively lower $\varepsilon Nd(T)$ values (0.9–3.1) in samples 01KD9, 01KD15A and 01KD16 are attributed to the various degrees of crustal contamination to the intra-plate basaltic magmas. Such Nb–Ta depletions, when taken alone, could lead to the inference to an island-arc origin (e.g. Zhou et al., 2002).

Sample 01KD11 is considered the least crustal-contaminated sample, showing a relatively high $\varepsilon Nd(T)$ value of 3.4 and insignificant Nb–Ta depletion. It is noted that this least crustal-contaminated sample displays trace element pattern very similar to those of tholeiites of mantle plume origin, such as the Hawaii tholeiites, the Karoo flood basalts and the Gairdner dyke swam (Fig. 7b; Zhao et al., 1994 and references therein). Therefore, geochemical and Nd isotopic characteristics indicate a likely mantle plume origin for these Kangding mafic dykes.

6. Comparison with other continents: evidence for a superplume?

We thus consider both episodes of Neoproterozoic bimodal magmatism as due to mantle plumes. In addition to the evidence presented in Li et al. (1999) and above, recent geochemical and petrological results from ca. 820 to 800 Ma rift magmatism in both western (Li et al., 2003) and northwestern (Ling et al., 2003) South China are consistent with them being related to a mantle plume. Current evidence thus permits a mantle plume origin for both episodes of Neoproterozoic bimodal magmatism in South China. The island-arc geochemical signatures of some rocks, as reported in Zhou et al. (2002), could have been inherited from arcs of no younger than 900 Ma in those regions, which ceased to operate with the termination of the Sibao Orogeny at ca. 1000–900 Ma (e.g. Ling et al., 2003; Li et al., 2002).

The magmatic episodes in South China (Fig. 8a) can be correlated with those in Australia (Fig. 8b), Laurentia (Fig. 8c), India (Fig. 8d), and southern Africa (Fig. 8e).

6.1. Australia

As indicated in Fig. 8b, Neoproterozoic magmatism in Australia mostly occurred in two major episodes also. The ca. 830–795 Ma episode in South China is matched by the 824 ± 4 Ma Amata Dyke Swarm in Central Australia (Sun and Sheraton, 1996), the 827 ± 6 Ma Gairdner Dyke Swarm and 827 ± 9 Ma Little Broken Hill gabbro in southeastern Australia (Wingate et al., 1998), the ca. 815–800 Ma lamprophyre dyke and kimberlite pipes in the Kimberley, northwestern Australia (Pidgeon et al., 1989), and the 802 ± 10 Ma Rook Tuff in the Adelaide Geosyncline

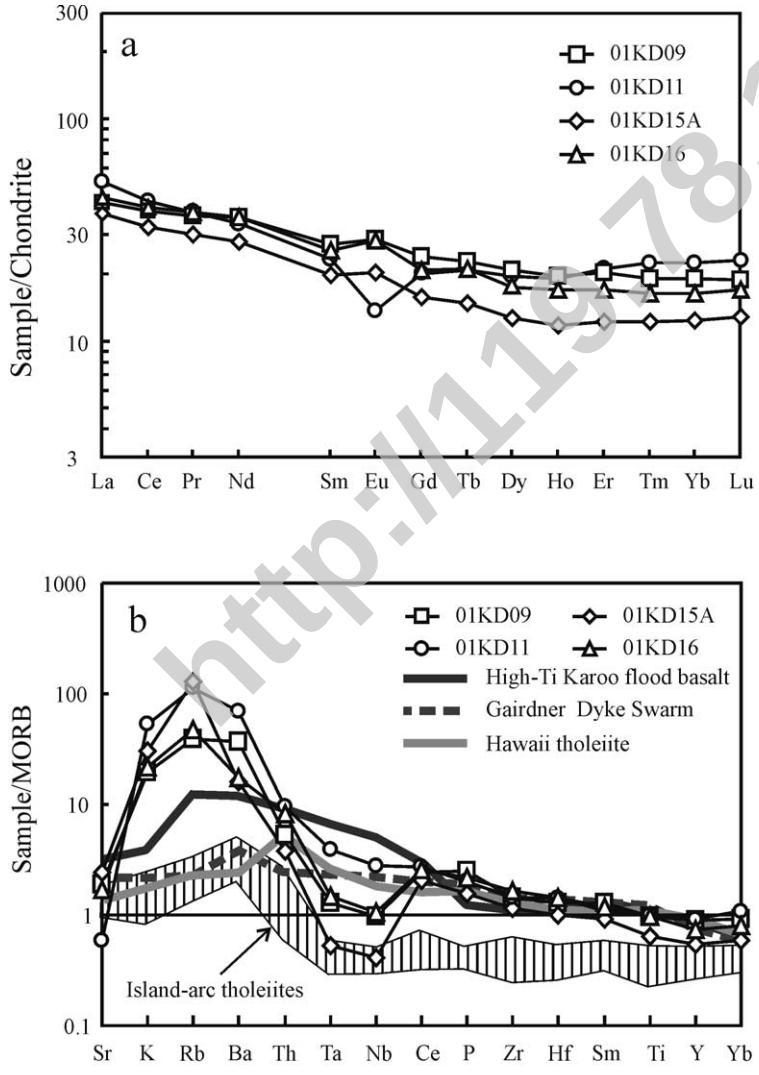

Fig. 7. REE (a) and trace element (b) pattens from mafic dykes in northern Kangdian Rift. The REE and trace element normalisation values are from Sun and McDonough (1989) and Pearce (1982), respectively. Pattern for the island-arc tholeiites is after Pearce (1983); average values of the high-Ti Karoo flood basalt, Gairdner dyke swarm and Hawaii tholeiite are from Duncan et al. (1990), Zhao et al. (1994) and Pearce (1983), respectively.

(Fanning et al., 1986). It is remarkable that even the two sub-peaks in South China, centred at ca. 825 and 800 Ma, respectively, are matched with those in the Australian data (Fig. 8a and b).

The 780–745 Ma episode is represented in Australia by the 777 ± 7 Ma Boucaut Volcanics in the Adelaide Geosyncline (C.M. Fanning, in Preiss, 2000), and the 755 ± 3 Ma Mundine Well Dyke Swarm in Western Australia (Wingate and Giddings, 2000). In addition, there is a 777 ± 7 Ma granitoid in northwestern Tasmania (Turner et al., 1998), and granitoids dated at 760 ± 12 and 748 ± 2 Ma on King Island, just north of Tasmania (Turner et al., 1998; Black et al., 1997). The origin of these granitoids and their apparent absence from mainland Australia had been an enigma for many geologists, but could be easily explained once

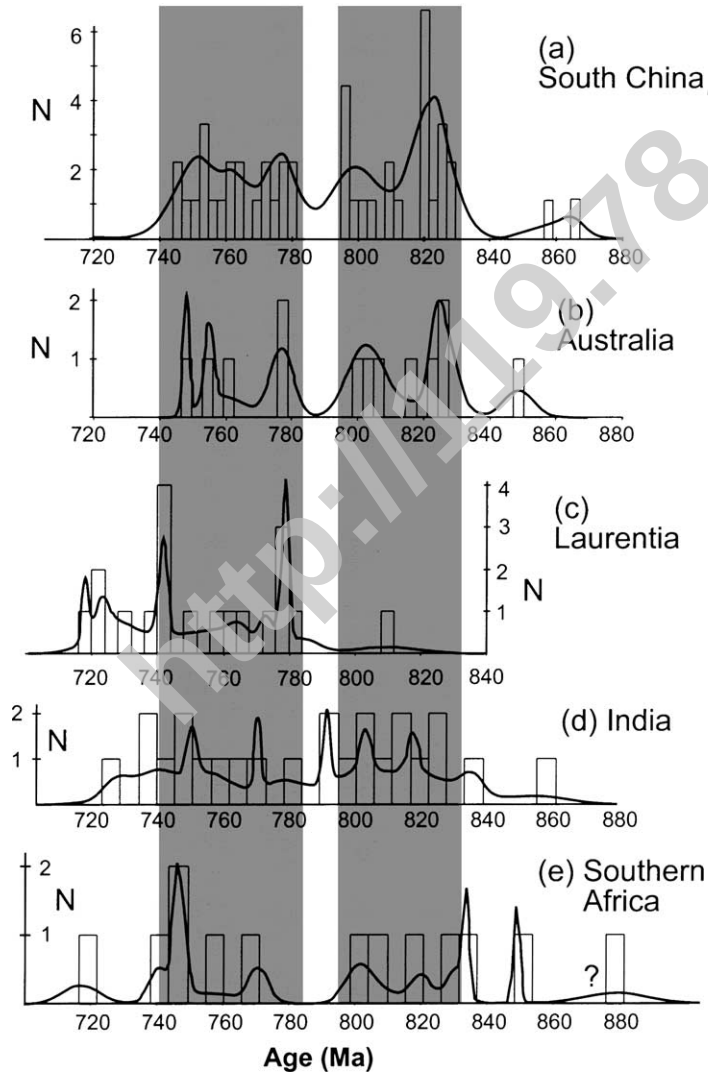

Fig. 8. Cumulative age spectra of Neoproterozoic igneous rocks in (a) South China, (b) Australia, (c) Laurentia, (d) India, and (e) Southern Africa. Sources for ages from continents other than South China are given in text.

they are treated as the counterparts of the similar-aged volcanic rocks in the mainland and products of crustal melting above a mantle plume (Li, 2001). As with the 830–795 Ma episode, the sub-peaks within the 780–745 Ma episode can also be roughly matched between South China and Australia (Fig. 8a and b).

The 827 ± 6 Ma Gairdner Dyke Swarm is found to be erosionally truncated by the Sturtian glacial deposits (760–700 Ma) (Preiss, 1987), indicating uplifting after the dyke intrusion. However, no direct contact between the dykes and the basal Adelaidean units has yet been found. There is nonetheless a continent-wide hiatus for the 1000–840 Ma interval in Australia (e.g. Walter and Veevers, 1997), which is consistent with the observation in South China. Moreover, geochemical and Nd isotope studies of Neoproterozoic sedimentary successions in southern-central Australia indicate a flood basalt province (Barovich and Foden, 2000), a likely result of syn-magmatic doming and erosion.

Ultramafic dykes with a 849 ± 9 Ma Rb–Sr age (phlogopite) has been reported in Norseman, Western Australia (Robey et al., 1989). If we accept this age as a reliable rock age, it can be correlated with the minor magmatic peak at ca. 860 Ma in South China.

6.2. Laurentia

Neoproterozoic magmatism in Laurentia mostly falls into the 780–720 Ma time range (Fig. 8c). Only the Sadlerochit-Shublik Mountains basalt in Alaska, dated at 810 ± 20 Ma using a Rb–Sr isochron (Clough et al., as cited in Rainbird et al., 1996), can be correlated with the 830–795 Ma episode in South China and Australia. The ca. 780 magmatism in Australia and South China is matched in western Laurentia by the 778 ± 3 Ma Little Dal quartz diorite plug in the Mackenzie Mountains (Jefferson and Parrish, 1989), and the ca. 780 Ma radiating mafic dyke swarms (Park et al., 1995). These mafic dyke swarms include the Tsezotene sills/dykes and the Hottah dykes in the Mackenzie Mountains, and the Tobacco Root Mountains dykes, Beartooth Mountains dykes and the Teton Range dykes in the Wyoming Province. Park et al. (1995) argued that the radiating dyke swarms point to a plume centre west of Laurentia in Rodinia (Fig. 1a).

The ca. 770–745 Ma magmatism in Australia and South China is matched in western Laurentia by magmatic activity along rift margins in both western and southeastern Laurentia (present coordinates). Along western Laurentia, there are the 740 ± 36 Ma Mount Copeland syenite gneiss (Parrish and Scammell, 1988) and the 741 ± 22 Ma Malton gneissic granite (Evenchick et al., 1984) in the southern Rocky Mountains, with the latter directly overlain by the Windermere rift successions. There were also the 751 ± 26 Ma Mount Harper Group rhyolite of northwest Canada (Roots and Parrish, 1988) and the 762 ± 44 Ma Huckleberry Formation volcanics of northern Washington (Devlin et al., 1988) at the basal parts of the rift successions (e.g. Rainbird et al., 1996). Although little attention has been previously paid to the Neoproterozoic granitic intrusions that often directly underlie the rift successions, their close temporal and spatial associations with the rift volcanism, and the lack of any convergent tectonics at the time, make them likely cogenetic with the rift volcanism. Furthermore, direct contact relationship between the similar-aged granitic rocks and the rift successions indicates syn-magmatic rapid crustal unroofing, a hallmark for plume-induced magmatism.

In southeastern Laurentia, the 770–745 Ma magmatism is represented by 765 ± 7 Ma alkali granites (Fetter and Goldberg, 1995), 741 ± 3 Ma bimodal plutonic rocks (Su, 1994), and 742 ± 2 Ma metarhyolites (Fetter and Goldberg, 1995) in the Blue Range province of southern Appalachians, and by 758 ± 12 Ma bimodal rift volcanics in Mount Rogers of Virginia (Aleinikoff et al., 1995). Fetter and Goldberg (1995) reported evidence arguing for a plume origin for these magmatic activities in eastern Laurentia. As in western Laurentia, the direct contact relationship between the 742 ± 2 Ma metarhyolites and the 765 ± 7 Ma alkali granites (Fetter and Goldberg, 1995) can again be explained by plume-induced crustal unroofing.

As shown in Fig. 8c, there is also a ca. 720 Ma magmatic episode in Laurentia (i.e. the Franklin igneous event), which Heaman et al. (1992) interpreted as of mantle plume origin related to the breakup between Laurentia and Siberia. However, this event is not present in either South China or Australia (Fig. 8a–c).

6.3. India, Seychelles and Madagascar

Neoproterozoic bimodal, anorogenic magmatism in India spans from ca. 860 to 730 Ma (Santosh et al., 1989; Radhakrishna and Mathew, 1996; Miyazaki et al., 2000; Chetty, 2001; Deb et al., 2001 and references therein; Kurian et al., 2001; Torsvik et al., 2001b). Their age distribution has one broad peak at ca. 840–790 Ma, another broad peak at ca. 780–730 Ma, and a possible minor peak at ca. 860 Ma (Fig. 1d). This broad pattern of age distribution is very similar to that of South China and Australia.

The rock types in India include alkaline granitoids (syenites), gabbros, mafic dykes, and bimodal (but dominantly felsic) volcanics such as those in the Malani igneous suite (e.g. Maheshwari et al., 2001; Roy, 2001). As on the other continents, there is also a hiatus between the middle to late Neoproterozoic successions and the underlying, pre-Neoproterozoic rocks (e.g. Chaudhuri et al., 2002), indicating possible plume-induced crustal doming and unroofing during the mid-Neoproterozoic.

Similar aged biomodal magmatic activites are also well developed in the Seychelles (Tucker et al., 2001;

Torsvik et al., 2001a) and in Madagascar (Handke et al., 1999; Kröner et al., 1999, 2000; Tucker et al., 1999). Handke et al. (1999) and Tucker et al. (2001) interpreted these igneous rocks, together with the Malani igneous suite in northwestern India, as of island arc origin because of their possible continental margin location in Rodinia. Others have argued that they were developed in an extentional environment (e.g. Kröner et al., 2000). Similar rocks exist in southern and eastern India also, away from the perceived continental margin location in Rodinia. The overall petrological and geochemical characters, and the lack of coeval island arc volcaniclastic rocks in those regions, make a mantle plume origin a more plausible interpretation.

6.4. Southern Africa

Igneous rocks in southern Africa also share a similar age distribution (e.g. Hanson et al., 1988, 1998; Frimmel et al., 1996, 2001; Hoffman et al., 1996; Frimmel and Frank, 1998; Rozendaal et al., 1999; Vinyu et al., 1999) (Fig. 8e). These rocks in places are clearly related to continental rift, and some have been interpreted as of mantle plume origin (e.g. Frimmel et al., 2001). In southwestern Africa, ca. 770 Ma syenites are unconformably overlain by rift successions no younger than 746 ± 2 Ma, again indicating rapid unroofing at the time of the magmatism.

6.5. Two independent episodes of plume breakout, or a mantle superplume?

As described above, there is evidence for mantle plume activity at both ca. 840–790 Ma and ca. 780–740 Ma during Rodinian time. Whereas the earlier episode was well developed in South China, Australia, India and southern Africa, the latter spread to the western and southern parts of Laurentia (Fig. 9).

Possible explanations for these magmatic epidoses are: (1) they are arc- or orogenesis-related (e.g. Li, 1999; Tucker et al., 2001; Zhou et al., 2002); (2) they are products of passive mantle upwelling beneath stretched and thinned continental lithosphere (e.g. White and McKenzie, 1989); (3) they are products of individual unrelated mantle plumes. However, the following observations argue not only for a plume origin, but also for the possible existence of a mantle

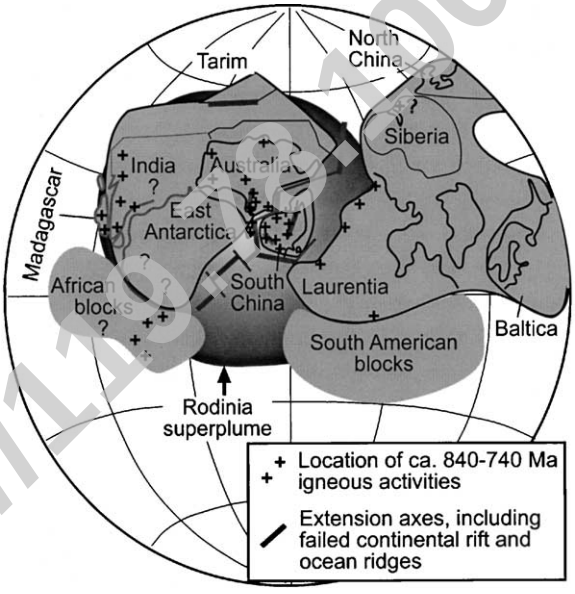

Fig. 9. A schematic diagram showing the proposed Neoproterozoic superplume beneath Rodinia. Locations of igneous activities discussed in the text are shown as crosses.

superplume under the supercontinent Rodinia, that eventually led to its breakup.

1. Geochemical and/or radiating patterns of mafic dyke swarms call for mantle plumes at both ca. 840–795 Ma and ca. 780–745 Ma, coinciding with the timing of rifting and breakup of Rodinia (e.g. Powell et al., 1994; Preiss, 2000; Wingate and Giddings, 2000; Wang and Li, 2003);
2. An early Neoproterozoic sedimentary hiatus is common in South China (Wang and Li, 2003), Australia (e.g. Walter and Veevers, 1997; Preiss, 2000), India (e.g. Chaudhuri et al., 2002), southern Africa (e.g. Frimmel et al., 2001), and possibly Laurentia (Rainbird et al., 1996) and East Antarctica. Together with evidence for syn-magmatic rapid unroofing in many of the continents (see discussions earlier), this suggests trans-Rodinia lithospheric doming and unroofing from ca. 860(?)–840 to ca. 740 Ma;
3. Widespread Neoproterozoic anorogenic, commonly bimodal magmatism on most of these continents demands a prolonged (from ca. 860 Ma to at least 745 Ma), trans-Rodinia mantle heat source, which can be readily provided by a superplume;

4. The common occurrence of alkali or peralkali granitoids is consistent with them being of interplate, possibly plume-related origin;
5. The occurrence of kimberlite pipes and lamprophyres in Western Australian cratons (Pidgeon et al., 1989) indicates a hot mantle beneath at least the Australian craton;
6. The common occurrence of anorogenic granitoids just prior to the rifting event in both South China (e.g. Li et al., 2003) and other continents (see discussions in Section 6) is inconsistent with them being the results of passive mantle upwelling beneath stretched and thinned continental lithosphere (e.g. White and McKenzie, 1989).

We envisage that, like the mantle superplume (or superswell, Anderson, 1982) developed underneath Panagea, the Rodinia superplume rose beneath the central and western parts of Rodinia, with a diameter of over 6000 km (Fig. 9). The superplume could have been shown as a number of normal plumes, like the ca. 825 and 780–745 Ma plume-heads just off South Australia (Zhao et al., 1994), and west of Laurentia (Park et al., 1995); both could have been beneath South China (Li et al., 1999; this study). This superplume could have caused broad doming over Rodinia, with its heat causing widespread anatectic melting. Continental rifting over the superplume could have eventually led to the breakup of Rodinia by ca. 750 Ma (e.g. Wingate et al., 1998; Li and Powell, 2001).

7. Conclusions

We report in this paper two major pulses of bimodal, anorogenic magmatic activity in South China during the Neoproterozoic: one during ca. 830–795 Ma, and the other during ca. 780–745 Ma. Whereas the latter phase occurred during the continental rifting, the earlier one started prior to the rifting and peaked at the beginning of the rifting at ca. 820 Ma. Geochemical data from mafic rocks of both episodes exhibit characteristics of magmas of mantle plume origin (Ling et al., 2003; Fig. 7 of this study), whereas the voluminous felsic rocks were mostly derived from crustal melting caused by the heat from the plumes. The plume origin for the magmatic activities is also supported by the continental-scale rapid, syn-magmatic lithospheric doming and unroofing, as seen by the depositional contact between the rift successions (≤820 Ma) and the widespread ca. 820 Ma granitoids (e.g. Li et al., 2003). There was also a minor pulse of magmatism at ca. 860 Ma, but its tectonic significance is as yet unclear.

The magmatic episodes in South China, along with its rift history, can be closely matched with those in Australia (e.g. Preiss, 2000; Wang and Li, 2003), and be broadly matched with igneous activities in Laurentia, India, and southern Africa (Fig. 8). In particular, South China could provide the missing record for both the ca. 825 Ma plume-head as suggested by the Gairdner dyke swarm in Australia (Zhao et al., 1994), and the ca. 780 plume-head as required by the radiating mafic dyke swarms in western Laurentia (Park et al., 1995). This interpretation thus supports the hypothesis by Li et al. (1995, 2002) that South China was between Australia and Laurentia in Rodinia.

Moreover, we propose the existence of a mantle superplume under the supercontinent Rodinia based on the following observations: (1) the trans-Rodinia distribution of the largely synchronous Neoproterozoic magmatic episodes that require an enormous heat source; (2) their common anorogenic and bimodal characteristics with some typical of mantle plume origin; (3) their common relationship with continental rifting (some before rifting); (4) the common pre- and syn-rift lithospheric doming and unroofing; (5) the prolonged (~100 Ma) duration of the magmatic and continental rifting events. The formation of the superplume may at least partly be due to the thermal insulation effect of the supercontinent. However, the doming above the superplume, the weakening effect on the lithosphere caused by the enormous heat conducted from the superplume and the prolonged and widespread magmatic activities, and the continental rifting, eventually led to the breakup of the supercontinent. This has remarkable similarities with the formation of the Pangaean superplume during the Permo-Carboniferous (e.g. Doblas et al., 1998) that led to its breakup in the Cretaceous. Superplumes may thus have played a major role in driving global plate tectonics since at least Neoproterozoic time.

Acknowledgements

This collaborative project was jointly supported by the Australian Research Council through the Tectonics Special Research Centre grant and ARC small and IREX grants, by the National Natural Science Foundation of China (grants No. 59810761886 and 40032010B), and by the Chinese Academy of Science (grant KZCX2-101). Zircon analyses were performed on the Western Australian SHRIMP II operated by a WA university-government consortium with ARC support. We thank many people who made our field trips successful and enjoyable. In particular, we wish to thank Xianhe Yang, Chaomin Bao, Daquan Ma, and Ligeng Zi for sharing with us their intimate knowledge of various field regions. The paper benefited from constructive comments by reviewers Sung-Tack Kwon and Changqian Ma, and by co-editor Moonsup Cho. This is Tectonics Special Research Centre publication No. 195, and a contribution to IGCP 440.

References

Aleinikoff, J.N., Zartman, R.E., Walter, M., Rankin, D.W., Lyttle, P.T., Burton, W.C., 1995. U–Pb ages of metarhyolites of the Catoctin and Mount Rogers formations, central and southern Appalachians; evidence for two pulses of Iapetan rifting. Am. J. Sci. 295, 428–454.

Anderson, D.L., 1982. Hotspots, polar wander, Mesozoic convection and the geoid. Nature 297, 391–393.

Anderson, D.L., 1994. Superplume or supercontinents? Geology 22, 39–42.

Barovich, K.M., Foden, J., 2000. A neoproterozoic flood basalt province in southern-central Australia: geochemical and Nd isotope evidence from basin fill. Precambrian Res. 100, 213–234.

Black, L.P., Seymour, D.B., Corbett, K.D., Cox, S.E., Streit, J.E., Bottrill, R.S., Calver, C.R., Everard, J.L., Green, G.R., McClenaghan, M.P., Pemberton, J., Taheri, J., Turner, N.J., 1997. Dating Tasmania's Oldest Geological Events. AGSO Record 1997/15, 57 pp.

Chaudhuri, A., Saha, D., Deb, G.K., Deb, S.P., Mukherjee, M.K., Ghosh, G., 2002. The Purana basins of southern Cratonic Province of India—a case for Mesoproterozoic fossil rifts. Gond. Res. 5, 23–33.

Chetty, T.R.K., 2001. The Eastern Ghats Mobile Belt, India: a collage of juxtaposed terranes? Gond. Res. 4, 319–328.

Dalziel, I.W.D., 1991. Pacific margins of Laurentia and East Antarctica–Australia as a conjugate rift pair: evidence and implications for an Eocambrian supercontinent. Geology 19, 598–601.

Deb, M., Thorpe, R.I., Krstic, D., Corfu, F., Davis, D.W., 2001. Zircon U–Pb and galena Pb isotope evidence for an approximate 1.0 Ga terrane constituting the western margin of the Aravalli–Delhi orogenic belt, northwestern India. Precambrian Res. 108, 195–213.

Devlin, W.J., Brueckner, H.K., Bond, G.C., 1988. New isotopic data and a preliminary age for volcanics near the base of the Windermere Supergroup, northeastern Washington, USA. Can. J. Earth Sci. 25, 1906–1911.

Doblas, M., Oyarzun, R., Lopez, R.J., Cebria, J.M., Youbi, N., Mahecha, V., Lago, M., Pocovi, A., Cabanis, B., 1998. Permo-carboniferous volcanism in Europe and Northwest Africa: a superplume exhaust valve in the centre of Pangaea? In: Kinnaird, J.A. (Ed.), Aspects of tensional magmatism. J. Afr. Earth Sci. 26, 89–99.

Duncan, A.R., Amstrong, R.A., Erlank, A.J., Marsh, J.S., Watkins, R.T., 1990. MORB-related dolerites associated with the final phases of Karoo basalt volcanism in southern Africa. In: Parker, A.J., Rickwood, P.C., Tucker, D.H. (Eds.), Mafic Dykes and Emplacement Mechanisms. Balkema, Rotterdam, pp. 119–129.

Evenchick, C.A., Parrish, R.R., Gabrielse, H., 1984. Precambrian gneiss and late proterozoic sedimentation in north-central British Columbia. Geology 12, 233–237.

Fanning, C.M., Ludwig, K.R., Forbes, B.G., Preiss, W.V., 1986. Single and multiple grain U–Pb zircon analysis for the early Adelaidean Rook Tuff, Willouran Ranges, South Australia. Abstr. Geol. Soc. Aust. 15, 71–72.

Fetter, A.H., Goldberg, S.A., 1995. Age and geochemical characteristics of bimodal magmatism in the Neoproterozoic Grandfather Mountain rift basin. J. Geol. 103, 313–326.

Frimmel, H.E., Frank, W., 1998. Neoproterozoic tectono-thermal evolution of the Gariep Belt and its basement, Namibia and South Africa. Precam. Res. 90, 1–28.

Frimmel, H.E., Kloetzli, U.S., Siegfried, P.R., 1996. New Pb–Pb single zircon age constraints on the timing of Neoproterozoic glaciation and continental break-up in Namibia. J. Geol. 104, 459–469.

Frimmel, H.E., Zartman, R.E., Späth, A., 2001. The Richtersveld Igneous Complex, South Africa: U–Pb zircon and geochemical evidence for the beginning of neoproterozoic continental breakup. J. Geol. 109, 493–508.

Ge, W.C., Li, X.H., Li, Z.X., Zhou, H.W., 2001. Mafic intrusions in Longsheng area: age and its geological implications. Chin. J. Geol. 36, 112–118 (in Chinese with English abstract).

Hacker, B.R., Ratschbacher, L., Webb, L., Ireland, T., Walker, D., Dong, S., 1998. U/Pb zircon ages constrain the architecture of the ultrahigh-pressure Qinling–Dabie Orogen, China. Earth Planet. Sci. Lett. 161, 215–230.

Hacker, B.R., Ratschbacher, L., Webb, L., McWilliams, M.O., Ireland, T., Calvert, A., Dong, S., Wenk, H.R., Chateigner, D., 2000. Exhumation of ultrahigh-pressure continental crust in east central China: Late Triassic-Early Jurassic tectonic unroofing. J. Geophys. Res. (B) 105, 13339–13364.

Handke, M.J., Tucker, R.D., Ashwal, L.D., 1999. Neoproterozoic continental arc magmatism in west-central Madagascar. Geology 27, 351–354.

Hanson, R.E., Wilson, T.J., Wardlaw, M.S., 1988. Deformed batholiths in the Pan-African Zambezi belt, Zambia: age and

implications for regional Proterozoic tectonics. Geology 16, 1134–1137.

Hanson, R.E., Hargrove, U.S., Martin, M.W., Bowring, S.A., Krol, M.A., Hodges, K.V., Munyanyiwa, H., Blenkinsop, T.G., 1998. New geochronological constraints on the tectonic evolution of the Pan-African Zambezi Belt, South Central Africa. J. Afr. Earth Sci. 27, 104–105.

Heaman, L.M., LeCheminant, A.N., Rainbird, R.H., 1992. Nature and timing of Franklin igneous events, Canada; implications for a late Proterozoic mantle plume and the break-up of Laurentia. Earth Planet. Sci. Lett. 109, 117–131.

Hoffman, P.F., 1991. Did the breakout of Laurentia turn Gondwanaland inside-out? Science 252, 1409–1412.

Hoffman, P.F., Hawkins, D.P., Isachsen, C.E., Bowring, S.A., 1996. Precise U–Pb zircon age for early Damaran magmatism in the Summas Mountains and Welwitschia inlier, northern Damara belt, Namibia. Commun. Geol. Surv. Namibia 11, 47–52.

Jefferson, C.W., Parrish, R.R., 1989. Late Proterozoic stratigraphy, U–Pb zircon ages, and rift tectonics, Mackenzie Mountains, northwestern Canada. Can. J. Earth Sci. 26, 1784–1801.

Kröner, A., Zhang, G.W., Sun, Y., 1993. Granulites in the Tongbai area, Qinling belt, China: geochemistry, petrology, single zircon geochronology, and implications for the tectonic evolution of eastern Asia. Tectonics 12, 245–255.

Kröner, A., Windley, B.F., Jaeckel, P., Brewer, T.S., Razakamanana, T., 1999. New zircon ages and geological significance for the evolution of the Pan-African orogen in Madacascar. J. Geol. Soc. Lond. 156, 1125–1135.

Kröner, A., Hegner, E., Collins, A.S., Windley, B.F., Brewer, T.S., Razakamanana, T., Pidgeon, R.T., 2000. Age and magmatic history of the Antananarivo Block, central Madagascar, as derived from zircon geochronology and Nd isotopic systematics. Am. J. Sci. 300, 251–288.

Kurian, P.J., Krishan, M.R., Nambiar, C.G., Murphy, B.V.S., 2001. Gravity field and subsurface geometry of the Kalpatta granite, South India and the tectonic significance. Gond. Res. 4, 105–111.

Larson, R.L., 1991. Latest pulse of Earth; evidence for a Mid-Cretaceous super plume. Geology 19, 547–550.

Li, J., 1991. Characteristics of Jinning–Chengjiang magmatic rocks and plate tectonic movements. In: Liu, H. (Ed.), The Sinian System in China. Science Press, Beijing, pp. 220–300.

Li, X.H., 1999. U–Pb zircon ages of granites from the southern margin of the Yangtze block: timing of the Neoproterozoic Jinning Orogeny in SE China and implications for Rodinia assembly. Precambrian Res. 97, 43–57.

Li, X.H., Li, Z.X., Zhou, H., Liu, Y., Kinny, P.D., 2002a. U–Pb zircon geochronology, geochemistry and Nd isotopic study of Neoproterozoic bimodal volcanic rocks in the Kangdian Rift of South China: implications for the initial rifting of Rodinia. Precambrian Res. 113, 135–154.

Li, X.H., Li, Z.X., Zhou, H., Liu, Y., Liang, X., Li, W., 2002b (in press). SHRIMP zircon U–Pb age, geochemistry and Nd isotope of the Guandaoshan granite in western Sichuan: petrogenesis and tectonic implications. Sci. in China (in Chinese).

Li, X.H., Li, Z.X., Ge, W., Zhou, H., Li, W., Liu, Y., Wingate, M.T.D., 2003. Neoproterozoic granitoids in South China: crustal melting above a mantle plume at ca. 825 Ma? Precambrian Res. 122, 45–83.

Li, Z.X., 2001. Understanding the Precambrian tectonic events in tasmania: clues from south China. Geol. Soc. Aust. Abst. 64, 110–111.

Li, Z.X., Powell, C.McA., 2001. An outline of the palaeogeographic evolution of the Australasian region since the beginning of the neoproterozoic. Earth-Sci. Rev. 53, 237–277.

Li, Z.X., Zhang, L., Powell, C.M., 1995. South China in Rodinia: part of the missing link between Australia–East Antarctica and Laurentia? Geology 23, 407–410.

Li, Z.X., Li, X.H., Kinny, P.D., Wang, J., 1999. The breakup of Rodinia: did it start with a mantle plume beneath South China? Earth Planet. Sci. Lett. 173, 171–181.

Li, Z.X., Li, X.H., Zhou, H., Kinny, P.D., 2002. Grenvillian continental collision in South China: new SHRIMP U–Pb zircon results and implications for the configuration of Rodinia. Geology 30, 163–166.

Ling, W., Gao, S., Zhang, B., Li, H., Liu, Y., 2003. Neoproterozoic tectonic evolution of Yangtze craton, South China: implications for amalgamation and break-up of Rodinia Supercontinent. Precambrian Res. 122, 111–140.

Ludwig, K.R., 2001. Users manual for Isoplot/Ex rev. 2.49. Berkeley Geochronology Centre Special Publication No. 1a, 56 pp.

Ma, G., Li, H., Zhang, Z., 1984. An investigation of the age limits of the Sinian System in South China. Bull. Yichang Inst. Geol. Mineral Res. 8, 1–29.

Ma, G., Zhang, Z., Li, H., Chen, P., Huang, Z., 1989. A geochronostratigraphical study of the Sinian System in Yangtze Platform. Bull. Yichang Inst. Geol. Mineral Res. 14, 83–124.

Maheshwari, A., Sial, A.N.C., Chittora, V.K., Cruz, M.J.M., 2001. Geochemistry and petrogenesis of Siwana peralkaline granites, West of Barmer, Rajasthan, India. Gond. Res. 4, 87–95.

Miyazaki, T., Miyazaki, T., Kagami, H., Shuto, K., Morikiyo, T., Mohan, V.R., Rajasekaran, C., 2000. Rb–Sr geochronology, Nd–Sr isotopes and whole rock geochemistry of Yelagiri and Sevattur syenites, Tamil Nadu, South India. Gond. Res. 3, 39–53.

Moores, E.M., 1991. Southwest U.S.–East Antarctic (SWEAT) connection: a hypothesis. Geology 19, 425–428.

Park, J.K., Buchan, K.L., Harlan, S.S., 1995. A proposed giant radiating dyke swarm fragmented by the separation of Laurentia and Australia based on paleomagnetism of ca. 780 Ma mafic intrusions in western North America. Earth Planet. Sci. Lett. 132, 129–139.

Parrish, R.R., Scammell, R.J., 1988. The age of the Mount Copeland syenite gneiss and its metamorphic zircons, Monashee Complex, southeastern Columbia, Radiogenic age and isotopic studies: report 2. Geol. Sur. Can. Paper 88-2, 21–28.

Pearce, J.A., 1982. Trace element characteristics of lavas from destructive plate boundaries. In: Thorpe, R.S. (Ed.), Andesites. Wiley, New York, pp. 528–548.

Pearce, J.A., 1983. Role of the sub-continental lithosphere in magma genesis at active continental margins. In: Hawkesworth, C.J., Norry, M.J. (Eds.), Continental Basalts and Mantle Xenoliths. Shiva Publishing, Nantwich, pp. 230–249.

Pearce, J.A., Norry, M.J., 1979. Petrogenetic implications of Ti, Zr, Y, and Nb variations in volcanic rocks. Contrib. Mineral Petrol. 69, 33–47.

Pidgeon, R.T., Smith, C.B., Fanning, C.M., 1989. Kimberlite and lamproite emplacement ages in Western Australia. In: Ross, J., et al. (Eds.), Kimberlites and Related Rocks Volume 1: Their Composition, Occurrence, Origin and Emplacement. Geol. Soc. Aust. Spec. Pub. Blackwell Scientific Publications, Carlton, pp. 382–391.

Powell, C.M., Preiss, W.V., Gatehouse, C.G., Krapez, B., Li, Z.X., 1994. South Australian record of a Rodinian epicontinental basin and its mid-Neoproterozoic breakup (approximately 700 Ma) to form the palaeo-Pacific Ocean. Tectonophysics 237, 113–140.

Preiss, W.V., 1987. The Adelaide Geosyncline—Late Proterozoic stratigraphy, sedimentation, paleontology, and tectonics. Geol. Surv. South Aust. Bull. 53, 438.

Preiss, W.V., 2000. The Adelaide Geosyncline of South Australia and its significance in Neoproterozoic continental reconstruction. Precambrian Res. 100, 21–63.

Radhakrishna, T., Mathew, J., 1996. Late Precambrian (850–800 Ma) palaeomagnetic pole for the south Indian shield from the Harohalli alkaline dykes: geotectonic implications for Gondwana reconstructions. Precambrian Res. 80, 77–87.

Rainbird, R.H., Jefferson, C.W., Young, G.M., 1996. The early Neoproterozoic sedimentary Succession B of northwestern Laurentia: correlations and paleogeographic significance. GSA Bull. 108, 454–470.

Robey, J.V.A., Bristow, J.W., Marx, M.R., Joyce, J., Danchin, R.V., Arnott, F., 1989. Alkaline ultrabasic dikes near Norseman, Western Australia. In: Ross, J., et al. (Eds.), Kimberlites and Related Rocks Volume 1: Their Composition, Occurrence, Origin and Emplacement. Geol. Soc. Aust. Spec. Pub. Blackwell Scientific Publications, Carlton, pp. 383–391.

Roger, F., Calassou, S., 1997. U–Pb geochronology on zircon and isotope geochemistry (Pb, Sr and Nd) of the basement in the Songpan–Ganzi fold belt (China). C.R. Acad. Sci. Ser. II 324, 819–826 (In French with English abstract).

Roots, C.F., Parrish, R.R., 1988. Age of the Mount Harper volcanic complex, southern Ogilvie Mountains, Yukon. Radiogenic age and isotope studies, Report 2. Geol Sur. Can. Paper 88-2, pp. 29–35.

Rowley, D.B., Xue, F., Tucker, R.D., Peng, Z.X., Baker, J., Davis, A., 1997. Ages of ultrahigh pressure metamorphism and protolith orthogneisses from the eastern Dabie Shan; U/Pb zircon geochronology. Earth Planet. Sci. Lett. 151, 191–203.

Roy, A.B., 2001. Neoproterozoic crustal evolution of Northwestern Indian Shield: implications on break up and assembly of supercontinents. Gond. Res. 4, 289–306.

Rozendaal, A., Gresse, P.G., Scheepers, R., Le Roux, L.R., 1999. Neoproterozoic to early Cambrian Crustal evolution of the Pan-African Saldania Belt, South Africa. Precambrian Res. 97, 303–323.

Santosh, M., Iyer, S.S., Vasconcellos, M.B.A., Enzweiler, J., 1989. Late Precambrian alkaline plutons in southwest India: geochronologic and rare-earth elements constraints on Pan-African magmatism. Lithos 24, 65–79.

Sichuan Bureau of Geology and Mineral Resources, 1991. Regional Geology of Sichuan Province (in Chinese with English summary). Geological Memoirs 23. Geological Publishing House, Beijing, 730 pp.

Sinclair, J.A., 2001. Petrology, geochemistry, and geochronology of the "Yanbian ophiolite suite", South China: implications for the western extension of the Sibao Orogen. Honours Thesis, The University of Western Australia, Perth, 69 pp. (plus appendixes).

Stacey, J.S., Kramers, J.D., 1975. Approximation of terrestrial lead isotope evolution by a two-stage model. Earth Planet. Sci. Lett. 26, 207–221.

Su, Q., 1994. Geochronological isotopic studies of late Proterozoic crosshore-type plutons in the Southern Appalachian Blue Ridge, North Carolina and Tennessee. Doctoral dissertation, University of North Carolina, Chapel Hill. Chapel Hill, NC, United States, 185 pp.

Sun, S.-S., McDonough, W.F., 1989. Chemical and isotopic systematics of oceanic basalt: implications for mantle composition and processes. In: Saunders, A.D., Norry, M.J. (Eds.), Magmatism in the Ocean Basins. Geol. Soc. Spec. Pub. No. 42, pp. 528–548.

Sun, S.-S., Sheraton, J.W., 1996. Geochemical and isotopic evolution. In: Glikson, A.Y., et al. (Eds.), Geology of the western Musgrave Block, central Australia, with particular reference to the mafic-ultramafic Giles Complex. Aust. Geol. Surv. Org. (AGSO) Bull. 239, 135–143.

Torsvik, T.H., Ashwal, L.D., Tucker, R.D., Eide, E.A., 2001a. Neoproterozoic geochronology and palaeogeography of the Seychelles microcontinent; the India link. Precambrian Res. 110, 47–59.

Torsvik, T.H., Carter, L.M., Ashwal, L.D., Bhushan, S.K., Pandit, M.K., Jamtveit, B., 2001b. Rodinia refined or obscured; palaeomagnetism of the Malani Igneous Suite (NW India). Precambrian Res. 108, 319–333.

Tucker, R.D., Ashwal, L.D., Handke, M.J., Hamilton, M.A., Le Grange, M., Rambeloson, R.A., 1999. U–Pb geochronology and isotope geochemistry of the Archean and Proterozoic rocks of north-central Madagascar. J. Geol. 107, 135–153.

Tucker, R.D., Ashwal, L.D., Torsvik, T.H., 2001. U–Pb geochronology of Seychelles granitoids; a Neoproterozoic continental arc fragment. Earth Planet. Sci. Lett. 187, 27–38.

Turner, N.J., Black, L.P., Kamperman, M., 1998. Dating of Neoproterozoic and Cambrian orogenies in Tasmania. Aust. J. Earth Sci. 45, 789–806.

Vinyu, M.L., Hanson, R.E., Martin, M.W., Bowring, S.A., Jelsma, H.A., Krol, M.A., Dirks, P.H.G.M., 1999. U–Pb and $^{40}Ar/^{39}Ar$ geochronological constraints on the tectonic evolution of the easternmost part of the Zambezi orogenic belt, Northeast Zimbabwe. Precambrian Res. 98, 67–82.

Walter, M.R., Veevers, J.J., 1997. Australian Neoproterozoic palaeogeography, tectonics, and supercontinental connections. AGSO J. Aust. Geol. Geophys. 17, 73–92.

Wang, J., Li, Z.X., 2003. History of Neoproterozoic rift basins in South China: implications for Rodinia breakup. Precambrian Res. 122, 141–158.

White, R., McKenzie, D., 1989. Magmatism at Rift zones: the generation of volcanic continental margins and flood basalts. J. Geophys. Res. 94, 7685–7729.

Wilson, M., 1989. Igneous Petrogenesis. Unwin Hyman, London, 466 pp.

Wingate, M.T.D., Giddings, J.W., 2000. Age and palaeomagnetism of the Mundine Well dyke swarm, Western Australia: implications for an Australia–Laurentia connection at 755 Ma. Precambrian Res. 100, 335–357.

Wingate, M.T.D., Campbell, I.H., Compston, W., Gibson, G.M., 1998. Ion microprobe U–Pb ages for Neoproterozoic-basaltic magmatism in south-central Australia and implications for the breakup of Rodinia. Precambrian Res. 87, 135–159.

Xue, F., Kröner, A., Reischmann, T., Lerch, F., 1996. Palaeozoic pre- and post-collision calc-alkaline magmatism in the Qinling orogenic belt, central China, as documented by zircon ages on granitoid rocks. J. Geol. Soc. Lond. 153, 409–417.

Xue, F., Rowley, D.B., Tucker, R.D., Peng, Z.X., 1997. U–Pb zircon ages of granitoid rocks in the North Dabie Complex, eastern Dabie Shan, China. J. Geol. 105, 744–753.

Zhao, D., 2001. Seismic structure and origin of hotspots and mantle plumes. Earth Planet. Sci. Lett. 192, 251–265.

Zhao, J.X., Malcolm, M.T., Korsch, R.J., 1994. Characterisation of a plume-related ~800 Ma magmatic event and its implications for basin formation in central-southern Australia. Earth Planet. Sci. Lett. 121, 349–367.

Zhou, M.F., Yan, D.P., Kennedy, A.K., Li, Y., Ding, J., 2002. SHRIMP U–Pb zircon geochronological and geochemical evidence for Neoproterozoic arc-magmatism along the western margin of the Yangtze Block, South China. Earth Planet. Sci. Lett. 196, 51–67.